On the active control of crack growth in elastic media

Patrick Hild* Arnaud Münch† Yves Ousset‡

April 24, 2008

Abstract

Let S be a 2-D elastic structure submitted to a fixed boundary load $\boldsymbol{f}$ and containing a crack γ. In the framework of the linear fracture theory, a common tool used to describe the smooth evolution of γ is the so-called energy release rate defined as the variation of the mechanical energy with respect to the crack dimension. Precisely, the well-known Griffith's criterion postulates the evolution of the crack if this rate - positive measure of the singularity which depends quadratically on the displacement field - reaches a critical value. In this work, we numerically investigate whether or not this rate may be reduced by applying an additional boundary load with a support disjoint from the support of the initial load $\boldsymbol{f}$ possibly responsible of the growth. We first introduce a well-posed relaxed formulation of this optimal location problem, and then compute explicitly the variation of the relaxed energy release rate with respect to the location of the additional force and also with respect to its intensity, taken into account the contact condition on the crack lips. Numerical simulations, based on a gradient descent method permit to optimize the support and amplitude of the extra load and so to reduce significantly the energy release rate. The optimal extra force highlights the balance between the opening and the in-plane shear modes. The case of a multi-crack structure is considered as well.

Key Words: Fracture mechanics, Optimal location problem, Relaxation.

1 Introduction - Problem statement

Since the seventies a huge literature has been devoted to the modelization of crack growth in elastic media, both on experimental, theoretical and numerical point of view. In this respect, many models and theories have been introduced and developed including linear fracture theory [19] and damage theory [4]. In the linear fracture framework, the different criteria used to described the crack growth may be divided into two categories: on one hand, we mention local (pointwise) criteria based on the information of the stress elasticity tensor (or displacement field) in the neighborhood of the crack tip. The growth may appear if a combination of the stress components (for instance the Von Mises stress) reaches a critical value. On the other hand, among energetic criteria, the

*Laboratoire de Mathématiques de Besançon, Université de Franche-Comté, UMR CNRS 6623, 16, route de Gray 25030 Besançon, France - patrick.hild@univ-fcomte.fr. Supported by grant ANR-05-JC-0182-01.

†Corresponding author - Laboratoire de Mathématiques de Besançon, Université de Franche-Comté, UMR CNRS 6623, 16, route de Gray 25030 Besançon, France - arnaud.munch@univ-fcomte.fr. Partially supported by grants ANR-05-JC-0182-01 and ANR-07-JC-183284.

‡Département Mécanique du Solide et de l'Endommagement, ONERA, 29, avenue de la Division Leclerc, BP 72, 92322, Chatillon, France.

well-known and still widely used to describe the static-crack growth is the criterion introduced in 1921 by Griffith [13]. Based on the energy release rate, this criterion has been recently revisited and reformulated into a minimum principle setting [12]. The energy release rate is defined as the variation of the elastic energy associated with a cracked structure with respect to the variation of the crack dimension. One may show that this quantity - usually denoted by G in the literature - is a strength and can be derived from a thermo-dynamic potential. Griffith has postulated the infinitesimal growth of the crack if this cracking strength reaches a critical value G_c, dependent coefficient of the material characteristics and experimentally evaluated:

-Griffith Criterion (1921)-

$$G(\text{material characteristics, loading configuration, shape}) > G_c \Longrightarrow \text{Crack growth.}$$

Both the Von Mises stress and the energy release rate depend on the kinematical displacement via mainly the material characteristics (elasticity tensor), the loading configuration and also the shape of the structure. In this respect, in order to prevent the growth, most of the developments have been focused on the design of new materials acting on the material characteristics to reduce the Von Mises stress or the cracking strength G. We mention the progress achieved with the composite materials. In parallel, there are by now strong developments in the field of "smart materials and systems". This generic terminology designates for instance adaptive structures with self-controlled mechanisms. Strain and electrical or magnetic fields couplings may be exploited to provide built-in feedback control (see [17] for some mathematical examples). The characteristic material being fixed, another mean in this spirit to reduce the energy release rate is to act on the loading configuration. This is the purpose of this work.

Let S be an elastic structure occupying a bounded domain Ω of $\mathbb{R}^2$ (referred to the orthonormal frame $(O, \boldsymbol{e_1}, \boldsymbol{e_2})$), fixed on a part $\Gamma_0 \subset \partial\Omega$ and submitted to a normal load $\boldsymbol{G} \in (L^2(\partial\Omega\backslash\Gamma_0))^2$ defined by

$$\boldsymbol{G} = \boldsymbol{f}\mathcal{X}_{\Gamma_f} + \boldsymbol{h}\mathcal{X}_{\Gamma_h},$$

where

$$\boldsymbol{f} \in (L^2(\Gamma_f))^2, \quad \boldsymbol{h} \in (L^2(\Gamma_h))^2, \quad \Gamma_f, \Gamma_h \subset \partial\Omega\backslash\Gamma_0, \quad \Gamma_f \cap \Gamma_h = \emptyset,$$

and $\mathcal{X}_{\Gamma_f} \in L^\infty(\Gamma_f, \{0,1\})$ denotes the characteristic function of Γ_f. The domain Ω contains a crack γ of extremity $\boldsymbol{F}$, unloaded (i.e., $\Gamma_f \cap \gamma = \emptyset$, $\Gamma_h \cap \gamma = \emptyset$) and free (i.e., $\Gamma_0 \cap \gamma = \emptyset$) as depicted in Figure 1. The corresponding displacement field $\boldsymbol{u} = (u_1, u_2)$ lies in the convex set

$$\mathbf{K} = \{\boldsymbol{v} \in (H^1_{\Gamma_0}(\Omega))^2, [\boldsymbol{v} \cdot \boldsymbol{\nu}] \leq 0 \text{ on } \gamma\} \tag{1}$$

where

$$H^1_{\Gamma_0}(\Omega) = \{v \in H^1(\Omega), v = 0 \text{ on } \Gamma_0\}.$$

In (1), the notation $[\boldsymbol{v} \cdot \boldsymbol{\nu}]$ represents the jump of the normal displacement field $\boldsymbol{v} \cdot \boldsymbol{\nu}$ across the crack γ. The sign condition of the jump describes the non-interpenetration of the crack lips. The symbol $\cdot$ stands for the inner product in $\mathbb{R}^2$ and $\boldsymbol{\nu}$ is the unit outward normal vector to $\partial\Omega$. The displacement field $\boldsymbol{u}$ minimizes at equilibrium the energy $J(., \gamma)$ on $\mathbf{K}$:

$$J(\boldsymbol{v}, \gamma) = \frac{1}{2}\int_\Omega Tr(\boldsymbol{\sigma}(\boldsymbol{v})\,\nabla\boldsymbol{v})dx - \int_{\Gamma_f} \boldsymbol{f} \cdot \boldsymbol{v}\, d\sigma - \int_{\Gamma_h} \boldsymbol{h} \cdot \boldsymbol{v}\, d\sigma \tag{2}$$

where Tr denotes the trace operator, i.e., $Tr(\boldsymbol{\sigma}(\boldsymbol{v})\,\nabla\boldsymbol{v}) = \sum_{i,j=1}^2 \sigma_{ij}(\boldsymbol{u})\partial u_j/\partial x_i$. As it is well-known, the unique field $\boldsymbol{u}$ solving (2) satisfies the following linear partial differential system (3)–(4):

$$\begin{cases} -\,\boldsymbol{div}\,\boldsymbol{\sigma}(\boldsymbol{u}) = 0 \quad \text{in} \quad \Omega, \qquad \boldsymbol{\sigma}(\boldsymbol{u}) \equiv \mathbb{A}\,\boldsymbol{\varepsilon}(\boldsymbol{u}), \quad \boldsymbol{\varepsilon}(\boldsymbol{u}) \equiv (\nabla\boldsymbol{u} + (\nabla\boldsymbol{u})^T)/2, \\ \boldsymbol{u} = 0 \quad \text{on} \quad \Gamma_0 \subset \partial\Omega, \qquad \boldsymbol{\sigma}(\boldsymbol{u})\boldsymbol{\nu} = \boldsymbol{f}\mathcal{X}_{\Gamma_f} + \boldsymbol{h}\mathcal{X}_{\Gamma_h} \quad \text{on} \quad \partial\Omega\backslash\Gamma_0 \end{cases} \tag{3}$$

where $\mathbb{A}$ stands for the 2-D elasticity tensor, and where the following conditions represent unilateral contact without friction on γ (see [18]):

$$[u_\nu] \equiv [\boldsymbol{u} \cdot \boldsymbol{\nu}] \leq 0, \quad \sigma_\nu \equiv (\boldsymbol{\sigma}(\boldsymbol{u})\boldsymbol{\nu}) \cdot \boldsymbol{\nu} \leq 0, \quad [u_\nu]\sigma_\nu = 0, \quad \boldsymbol{\sigma}(\boldsymbol{u})\boldsymbol{\nu} - \sigma_\tau \boldsymbol{\nu} = 0. \tag{4}$$

In the sequel, we introduce the notation

$$\Gamma = \partial\Omega \backslash (\Gamma_0 \cup \Gamma_f \cup \gamma).$$

In order to reduce the energy release rate (precisely defined in Section 2), one may act on the boundary load $\boldsymbol{G}$. In this respect, assuming fixed the main load $\boldsymbol{f}$ and its support Γ_f, we consider, for any $L \in (0,1)$, the following nonlinear problem:

$$(P_{\Gamma_h}): \quad \inf_{\mathcal{X}_{\Gamma_h} \in \mathcal{X}_L} G(\boldsymbol{u}, \boldsymbol{h}, \mathcal{X}_{\Gamma_h}); \quad \mathcal{X}_L = \{\mathcal{X} \in L^\infty(\Gamma, \{0,1\}), \|\mathcal{X}\|_{L^1(\Gamma)} = L\|\mathcal{X}_\Gamma\|_{L^1(\Gamma)}\}. \tag{5}$$

For any fixed $\boldsymbol{h}$ fixed in $(L^2(\Gamma_h))^2$, (P_{Γ_h}) is an optimal design problem which consists in finding the optimal distribution of the support $\Gamma_h \subset \Gamma$ of the additional load $\boldsymbol{h}$. Remark that the support Γ_h may *a priori* be composed of several disjoint components. On the other hand, the support $\Gamma_h \subset \Gamma$ of the additional force being fixed, one may also consider the following problem:

$$(P_h): \inf_{\boldsymbol{h} \in (L^2_L(\Gamma_h))^2} G(\boldsymbol{u}, \boldsymbol{h}, \mathcal{X}_{\Gamma_h}); (L^2_L(\Gamma_h))^2 = \{\boldsymbol{h} \in (L^2(\Gamma_h))^2, \|\boldsymbol{h}\|_{(L^2(\Gamma_h))^2} = L\|\boldsymbol{f}\|_{(L^2(\Gamma_f))^2}\}, \tag{6}$$

which consists in optimizing the amplitude of $\boldsymbol{h}$ in order to reduce G and therefore preventing the crack growth.

Problems (P_{Γ_h}) and (P_h) are two examples of optimal control problems. To the knowledge of the authors, the control of the crack growth by the boundary of the domain has not been investigated so far. Let us mention two preliminary notes by P. Destuynder ([8, 9]), on a similar problem for the Laplace operator. In [8], the author considers the dynamic wave equation posed on a 2D cracked domain and defines a growth criterion based on the stress intensity factor. A formulation for the derivative of this criterion is given with respect to a control defined on the boundary of the domain. On the other hand, reference [9] considers a stationary loaded structure with a crack and suggests a computational method for a control law which restricts the crack evolution (we refer to [10] for some numerical treatments). We also mention the recent work [25] where the authors study the possibility to annihilate the singularity in a crack domain using additional (singular !) boundary loads.

The aim of this paper is to solve numerically the nonlinear problems (P_{Γ_h}) and (P_h) using a gradient descent algorithm. The outline is as follows. Section 2 is devoted to a precise overview about the rate G and the way to compute it efficiently using surface integrals. In Section 3, we prove that problem (P_{Γ_h}) is well-posed when Γ_h possesses a finite number of disjoint components (Proposition 3.1) and then provided a well-posed relaxation (RP_{Γ_h}) in the general case (Theorem 3.1). Then, in Section 4, the first derivatives of the release rate with respect to Γ_h and $\boldsymbol{h}$ are computed explicitly which permits to characterize the minima of the relaxed problem, in terms of the solution of an adjoint problem (Theorem 4.1) and then to define a gradient descent algorithm. Section 5 presents several numerical experiments highlighting the efficiency of the approach. Finally, we point out some perspectives in Section 6.

The results detailed in this paper were partially announced in [16].

2 Overview about the energy release rate

In this section, we recall the definition of the energy release rate G and its expression in terms of surface integrals. We use the notation $\psi_{,i}$ for $\partial\psi/\partial x_i$, $i = 1, 2$ as well as the convention of summation of repeated indices.

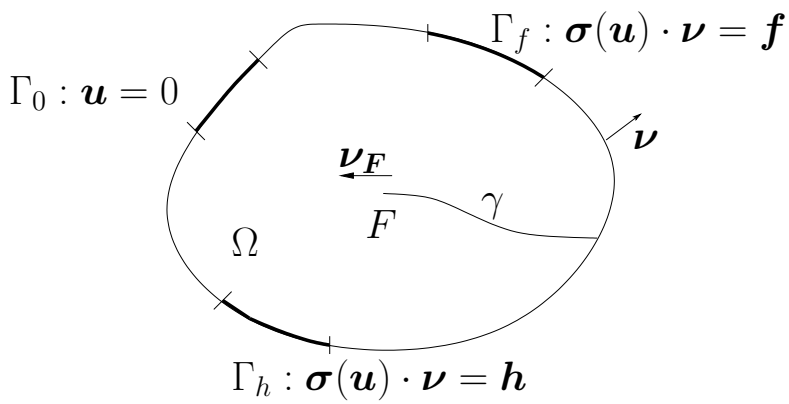

Figure 1: Illustration of the problem (P_{Γ_h}): Optimization of the location of Γ_h, the support of the extra load $\boldsymbol{h}$ in order to minimize the energy release rate.

In order to simplify the study, we assume that the crack γ remains rectilinear in the neighborhood of $\boldsymbol{F}$ and (without loss of generality) oriented along $\boldsymbol{e_1}$. We introduce a velocity field $\boldsymbol{\psi} = (\psi_1(x_1, x_2), 0) \in \mathbf{W} \equiv \{\boldsymbol{\psi} \in (W^{1,\infty}(\Omega, \mathbb{R}))^2, \boldsymbol{\psi} = 0 \text{ on } \partial\Omega\backslash\gamma\}$ and let η be in $\mathbb{R}^+$. Introducing the transformation $\mathcal{F}^\eta : \boldsymbol{x} \to \boldsymbol{x} + \eta\boldsymbol{\psi}(\boldsymbol{x})$ so that $\mathcal{F}^\eta(\boldsymbol{F}) = \boldsymbol{F^\eta}$ and $\mathcal{F}^\eta(\gamma) = \gamma^\eta$, we first recall the following definition.

Definition 2.1 (Energy release rate) *The derivative of the functional $-J(\boldsymbol{u}, \gamma)$ with respect to a variation of γ in the direction $\boldsymbol{\psi}$ is defined as the Fréchet derivative in $\mathbf{W}$ at 0 of the function $\eta \to -J(\boldsymbol{u}, (Id + \eta\boldsymbol{\psi})(\gamma))$, i.e.*

$$J(\boldsymbol{u}, (Id + \eta\boldsymbol{\psi})(\gamma)) = J(\boldsymbol{u}, \gamma) - \eta \frac{\partial J(\boldsymbol{u}, \gamma)}{\partial \gamma}.\boldsymbol{\psi} + o(\eta^2).$$

In the sequel, we denote by $g_{\boldsymbol{\psi}}(\boldsymbol{u}, \boldsymbol{h}, \mathcal{X}_{\Gamma_h})$ this derivative. ■

The procedure to obtain the explicit expression of $g_{\boldsymbol{\psi}}$ is technical but by now well-known (see [11, 21, 22]). Since the problem is self-adjoint, the derivative may be expressed in terms of $\boldsymbol{u}$ only:

Lemma 2.1 *The first derivative of $-J$ with respect to γ in the direction $\boldsymbol{\psi} = (\psi_1, 0) \in \mathbf{W}$ is given by*

$$\begin{aligned} g_{\boldsymbol{\psi}}(\boldsymbol{u}, \boldsymbol{h}, \mathcal{X}_{\Gamma_h}) &= -\frac{1}{2}\int_\Omega Tr(\boldsymbol{\sigma}(\boldsymbol{u})\,\nabla\boldsymbol{u})\,div\,\boldsymbol{\psi} dx + \int_\Omega Tr(\boldsymbol{\sigma}(\boldsymbol{u})\,\nabla\boldsymbol{u}\,\nabla\boldsymbol{\psi}) dx \\ &= -\frac{1}{2}\int_\Omega \sigma_{ij} u_{j,i} \psi_{1,1} dx + \int_\Omega \sigma_{ij} u_{j,1} \psi_{1,i} dx \end{aligned} \tag{7}$$

where $\boldsymbol{u} = \boldsymbol{u}(\boldsymbol{f}, \mathcal{X}_{\Gamma_f}, \boldsymbol{h}, \mathcal{X}_{\Gamma_h})$ is the solution of (3)–(4). ■

Moreover, as it is usual, the first derivative depends on the function $\boldsymbol{\psi}$ only in a neighborhood of the crack tip $\boldsymbol{F}$: this permits to link the derivative $g_{\boldsymbol{\psi}}$ defined on Ω with the thermo-dynamic strength G (locally defined on $\boldsymbol{F}$).

Lemma 2.2 *[(Local) Energy release rate] Let $C(\boldsymbol{F}, r)$ be the circle of center $\boldsymbol{F}$ and radius $r > 0$ and*

$$G_r(\boldsymbol{u}, \boldsymbol{h}, \mathcal{X}_{\Gamma_h}) = \frac{1}{2}\int_{C(\boldsymbol{F},r)} \sigma_{ij}(\boldsymbol{u}) u_{j,i} \psi_1 \nu_1 d\sigma - \int_{C(\boldsymbol{F},r)} \sigma_{kj}(\boldsymbol{u}) u_{j,1} \psi_1 \nu_k d\sigma;$$

then the thermo-dynamic strength G is linked to $g_{\boldsymbol{\psi}}$ as follows:

$$g_{\boldsymbol{\psi}}(\boldsymbol{u},\boldsymbol{h},\mathcal{X}_{\Gamma_h}) = \lim_{r\to 0} G_r(\boldsymbol{u},\boldsymbol{h},\mathcal{X}_{\Gamma_h})\ (\boldsymbol{\psi}\cdot\boldsymbol{\nu})_{|\boldsymbol{F}} \equiv G(\boldsymbol{u},\boldsymbol{h},\mathcal{X}_{\Gamma_h})\ \boldsymbol{\psi}(\boldsymbol{F})\cdot\boldsymbol{\nu}(\boldsymbol{F}), \quad \forall \boldsymbol{\psi}\in\mathbf{W}. \tag{8}$$

■

Remark 1 • *It follows from (8) that the energy release rate is*

$$G(\boldsymbol{u},\boldsymbol{h},\mathcal{X}_{\Gamma_h}) = g_{\boldsymbol{\psi}}(\boldsymbol{u},\boldsymbol{h},\mathcal{X}_{\Gamma_h}), \quad \forall \boldsymbol{\psi}\in\mathbf{W}\ s.t.\ \boldsymbol{\psi}(\boldsymbol{F})\cdot\boldsymbol{\nu}(\boldsymbol{F}) = 1. \tag{9}$$

Moreover, since only the derivatives of $\boldsymbol{\psi} = (\psi_1, 0)$ are involved in $g_{\boldsymbol{\psi}}$ defined by (7), it is more accurate from a numerical point of view to consider a function ψ_1 such that $\psi_1\nu_{F,1} = 1$ and constant in a neighborhood of $\boldsymbol{F}$. This permits to obtain the strength G with the relation (7) only function of the solution $\boldsymbol{u}$ far away from $\boldsymbol{F}$ where it is singular [11]. A simple choice is given by the radial function

$$\psi_1(\boldsymbol{x}) = \zeta(dist(\boldsymbol{x},\boldsymbol{F})), \quad \forall \boldsymbol{x}\in\Omega, \tag{10}$$

where the function $\zeta\in C^1(\mathbb{R}^+;[0,1])$ is defined as follows:

$$\zeta(r) = \begin{cases} 1 & r\le r_1 \\ \dfrac{(r-r_2)^2(3r_1-r_2-2r)}{(r_1-r_2)^3} & r_1\le r\le r_2 \\ 0 & r\ge r_2 \end{cases}$$

with $0 < r_1 < r_2 < dist(\partial\Omega\backslash\gamma,\boldsymbol{F}) = \inf_{\boldsymbol{x}\in\partial\Omega\backslash\gamma} dist(\boldsymbol{x},\boldsymbol{F})$. The equivalence (9) permits to use the expression (7) in (5) and (6).

- *It is crucial to note that the analytical expression (7) remains valid when the (frictionless) contact occurs on the crack lips γ (see [7]).*
- *The energy release rate is a measure of the singularity of $\boldsymbol{u}$ at the crack tip $\boldsymbol{F}$: precisely, the rate is related to the stress intensity factors K_I and K_{II} as follows :*

$$G(\boldsymbol{u},\boldsymbol{h},\mathcal{X}_{\Gamma_h}) = f(\boldsymbol{A})(K_I^2 + K_{II}^2)$$

where $f(\boldsymbol{A})$ is a scalar function of the elasticity tensor (see [11, 19]). Moreover, G is positive but not definite positive ($\boldsymbol{u} = 0$ implies that $G(\boldsymbol{u},\boldsymbol{h},\mathcal{X}_{\Gamma_h}) = 0$ but the converse is not true) so that the kernel of G: $Ker\,G = \{\boldsymbol{u}\in(H^1_{\Gamma_0}(\Omega))^2, G(\boldsymbol{u},\boldsymbol{h},\mathcal{X}_{\Gamma_h}) = 0\}$ is not reduced to zero. Then, ideally, problems (P_{Γ_h}) and (P_h) consist in determining Γ_h and $\boldsymbol{h}$ so that $\boldsymbol{u}(\boldsymbol{h},\mathcal{X}_{\Gamma_h})\in Ker\,G$. Reference [25] shows that a singular additional force allows to cancel the singularity at $\boldsymbol{F}$ (i.e., allows $K_I = K_{II} = 0$). ■

3 Well-posedness and relaxation of the problem (P_{Γ_h})

The optimal nonlinear location problem (P_{Γ_h}) is a prototype of ill-posed problem in the sense that the infimum may be not reached in the class $\mathcal{X}_L$ of characteristic functions: the optimal domain Γ_h may then be composed of an infinite number of disjoints components (we refer to [6, 14] and the references therein where several ill-posed problems are studied). The well-posed property is then recovered for instance if we assume that the number of disjoint components in Γ_h is finite:

PROPOSITION 3.1 *Let $\boldsymbol{h} \neq 0$ be fixed in $(L^2(\Gamma))^2$. If Γ_h is composed of a finite number of disjoint components, then problem (P_{Γ_h}) admits at least a solution.* ■

Proof. Without loss of generality, let us assume that Γ_h is composed of only one part. The energy release rate G is non-negative. This is direct consequence of the fact that $J(\boldsymbol{u}(\gamma_1), \gamma_1) \leq J(\boldsymbol{u}(\gamma_2), \gamma_2)$ when the crack γ_1 contains the crack γ_2, i.e. $\gamma_2 \subset \gamma_1$. The existence of a minimizer is then related to the continuity of G - or similarly from (8) of $g_{\boldsymbol{\psi}}$ - with respect to the variation of Γ_h on $\partial\Omega$ for a given metric of $\mathbb{R}$. Let us consider the Hausdorff distance (see [6]):

$$d^{\mathcal{H}}(\gamma_1, \gamma_2) = \sup(\mathrm{dist}_{\boldsymbol{x_1} \in \gamma_1}(x_1, \gamma_2), \mathrm{dist}_{\boldsymbol{x_2} \in \gamma_2}(x_2, \gamma_1)), \quad \forall \gamma_1, \gamma_2 \subset \Gamma,$$

and a minimizing sequence $(\Gamma_h^n)_{n \geq 0}$ of $\partial\Omega$ for $g_{\boldsymbol{\psi}}$ such that $d^{\mathcal{H}}(\Gamma_h^n, \Gamma_h) \to 0$ as n goes to infinity. The solution $\boldsymbol{u}^n \in (H^1_{\Gamma_0}(\Omega))^2$ associated with Γ_h^n satisfies the formulation

$$\int_\Omega \mathrm{Tr}(\boldsymbol{\sigma}(\boldsymbol{u^n}) \nabla \boldsymbol{v}) dx = \int_{\Gamma_f} \boldsymbol{f} \cdot \boldsymbol{v} d\sigma + \int_{\Gamma_h^n} \boldsymbol{h} \cdot \boldsymbol{v} d\sigma, \quad \forall \boldsymbol{v} \in (H^1_{\Gamma_0}(\Omega))^2. \tag{11}$$

Assuming $\boldsymbol{h} \in (L^2(\Gamma_h^n))^2$ for all n, we have in particular for $\boldsymbol{v} = \boldsymbol{u^n}$

$$\int_\Omega \mathrm{Tr}(\boldsymbol{\sigma}(\boldsymbol{u^n}) \nabla \boldsymbol{u^n}) dx = \int_{\Gamma_f} \boldsymbol{f} \cdot \boldsymbol{u^n} d\sigma + \int_{\Gamma_h^n} \boldsymbol{h} \cdot \boldsymbol{u^n} d\sigma.$$

From the Korn inequality, there exists a positive constant C such that

$$\|\boldsymbol{u^n}\|_{(H^1_{\Gamma_0}(\Omega))^2} \leq C(\|\boldsymbol{h}\|_{(L^2(\Gamma_h^n))^2} + \|\boldsymbol{f}\|_{(L^2(\Gamma_f))^2}). \tag{12}$$

Moreover, the convergence of Γ_h^n towards Γ_h for the Hausdorff distance implies that $\|\boldsymbol{h}\|_{(L^2(\Gamma_h^n))^2} - \|\boldsymbol{h}\|_{(L^2(\Gamma_h))^2} \to 0$ as $n \to \infty$ (see [6]). Consequently, the sequence $(\boldsymbol{u^n})_n$ is uniformly bounded in the reflexive space $(H^1_{\Gamma_0}(\Omega))^2$ and one may extract a subsequence (still denoted by $\boldsymbol{u^n}$) such that $\boldsymbol{u^n}$ weakly converges to $\boldsymbol{u^\star}$ in $(H^1_{\Gamma_0}(\Omega))^2$. By passing to the limit in (11), $\boldsymbol{u^\star}$ verifies the formulation:

$$\int_\Omega \mathrm{Tr}(\boldsymbol{\sigma}(\boldsymbol{u^\star}) \nabla \boldsymbol{v}) dx = \int_{\Gamma_f} \boldsymbol{f} \cdot \boldsymbol{v} d\sigma + \int_{\Gamma_h} \boldsymbol{h} \cdot \boldsymbol{v} d\sigma, \quad \forall \boldsymbol{v} \in (H^1_{\Gamma_0}(\Omega))^2.$$

Now, observe that the compact embedding of the trace operator $tr : H^{1/2}(\partial\Omega) \to L^2(\partial\Omega)$ implies that the trace $tr(\boldsymbol{u^n})_{|\Gamma_h}$ converges to $tr(\boldsymbol{u^\star})_{|\Gamma_h}$ in $(L^2(\Gamma_h))^2$. Therefore,

$$\begin{aligned} \int_\Omega Tr(\boldsymbol{\sigma}(\boldsymbol{u^n}) \nabla \boldsymbol{u^n}) dx &= \int_{\Gamma_f} \boldsymbol{f} \cdot \boldsymbol{u^n} d\sigma + \int_{\Gamma_h^n} \boldsymbol{h} \cdot \boldsymbol{u^n} d\sigma \\ &= \int_{\Gamma_f} \boldsymbol{f} \cdot \boldsymbol{u^n} d\sigma + \int_{\Gamma_h^n} \boldsymbol{h} \cdot (\boldsymbol{u^n} - \boldsymbol{u^\star}) d\sigma + \int_{\Gamma_h^n} \boldsymbol{h} \cdot \boldsymbol{u^\star} d\sigma \end{aligned}$$

converges towards $\int_{\Gamma_f} \boldsymbol{f} \cdot \boldsymbol{u^\star} d\sigma + \int_{\Gamma_h} \boldsymbol{h} \cdot \boldsymbol{u^\star} d\sigma$. Then, using that $\int_\Omega Tr(\boldsymbol{\sigma}(\boldsymbol{u^n}) \nabla \boldsymbol{u^\star}) dx \to \int_\Omega Tr(\boldsymbol{\sigma}(\boldsymbol{u^\star}) \nabla \boldsymbol{u^\star}) dx$ and $Tr(\boldsymbol{\sigma}(\boldsymbol{u^\star}) \nabla \boldsymbol{u^n}) = Tr(\boldsymbol{\sigma}(\boldsymbol{u^n}) \nabla \boldsymbol{u^\star})$, we obtain from the equality

$$\begin{aligned} \int_\Omega Tr(\boldsymbol{\sigma}(\boldsymbol{u^n} - \boldsymbol{u^\star}) \nabla (\boldsymbol{u^n} - \boldsymbol{u^\star})) dx &= \int_\Omega Tr(\boldsymbol{\sigma}(\boldsymbol{u^\star}) \nabla \boldsymbol{u^\star}) dx \\ &- 2 \int_\Omega Tr(\boldsymbol{\sigma}(\boldsymbol{u^\star}) \nabla \boldsymbol{u^n}) dx + \int_\Omega Tr(\boldsymbol{\sigma}(\boldsymbol{u^n}) \nabla \boldsymbol{u^n}) dx \end{aligned}$$

that $\int_\Omega Tr(\boldsymbol{\sigma}(\boldsymbol{u^n} - \boldsymbol{u^\star}) \nabla (\boldsymbol{u^n} - \boldsymbol{u^\star})) dx \to 0$ as $n \to 0$. Consequently, the sequence $\boldsymbol{u^n}$ converges strongly towards $\boldsymbol{u^\star}$ in $(H^1_{\Gamma_0}(\Omega))^2$. In view of (7), we conclude to the convergence of the decreasing sequence $g_{\boldsymbol{\psi}}(\boldsymbol{u}, \boldsymbol{h}, \mathcal{X}_{\Gamma_h^n})$ towards $g_{\boldsymbol{\psi}}(\boldsymbol{u}, \boldsymbol{h}, \mathcal{X}_{\Gamma_h})$. □

Without geometrical condition on Γ_h, a relaxation of (P_{Γ_h}) is *a priori* needed. Following recent developments in [23] on a similar problem, we now give a well-posed formulation of (P_{Γ_h}): let us introduce the following problem :

$$(RP_{\Gamma_h}): \quad \inf_{s\in S_L} g_{\boldsymbol{\psi}}(\boldsymbol{u},\boldsymbol{h},s); \quad S_L=\{s\in L^\infty(\Gamma,[0,1]), \|s\|_{L^1(\Gamma)}=L\|\mathcal{X}_\Gamma\|_{L^1(\Gamma)}\}$$

where $L\in(0,1)$ is the real parameter which appears in (5), and $\boldsymbol{u}$ the solution of

$$\begin{cases} -\,\boldsymbol{div}\,\boldsymbol{\sigma}(\boldsymbol{u})=0 \quad \text{in} \quad \Omega, \qquad \boldsymbol{\sigma}(\boldsymbol{u})\equiv\mathbb{A}\,\boldsymbol{\varepsilon}(\boldsymbol{u}), \quad \boldsymbol{\varepsilon}(\boldsymbol{u})\equiv(\nabla\boldsymbol{u}+(\nabla\boldsymbol{u})^T)/2, \\ \boldsymbol{u}=0 \quad \text{on} \quad \Gamma_0\subset\partial\Omega, \qquad \boldsymbol{\sigma}(\boldsymbol{u})\boldsymbol{\nu}=\boldsymbol{f}\mathcal{X}_{\Gamma_f}+s(\boldsymbol{x})\boldsymbol{h}\mathcal{X}_\Gamma \quad \text{on} \quad \partial\Omega\backslash\Gamma_0 \end{cases} \tag{13}$$

and (4). Observe that this new problem is obtained from the original one (P_{Γ_h}) simply by replacing the set of characteristic functions $\{\mathcal{X}_{\Gamma_h}\in L^\infty(\Gamma,\{0,1\})\}$ by its convex hull for the L^∞ weak-$\star$ topology, i.e., the set of densities $\{s\in L^\infty(\Gamma,[0,1])\}$. We obtain the following result:

THEOREM 3.1 *The problem (RP_{Γ_h}) is a full well-posed relaxation of (P_{Γ_h}) in the following sense:*

- *The problem (RP_{Γ_h}) is well-posed;*
- *The minimum of (RP_{Γ_h}) equals the infimum of (P_{Γ_h});*
- *Moreover, to the optimal density s^{opt} solution of (RP_{Γ_h}), one may associate [through a Young measure process] a minimizing sequence $(\Gamma_h^{(k)})_{(k>0)}$ for the problem (P_{Γ_h}), i.e., such that*

  (i) $\|\mathcal{X}_{\Gamma_h^{(k)}}\|_{L^1(\Gamma)}=\|s^{opt}\|_{L^1(\Gamma)}=L|\Gamma|, \quad \forall k>0,$

  (ii) $\lim_{k\to\infty} g_{\boldsymbol{\psi}}(\boldsymbol{u},\boldsymbol{h},\mathcal{X}_{\Gamma_h^{(k)}})=g_{\boldsymbol{\psi}}(\boldsymbol{u},\boldsymbol{h},s^{opt}).$ ■

Stectch of the proof - Observe that this result is natural since the location Γ_h appears only in the lower order part of the elliptic state equation (in contrast to standard optimal problems (see [27]) where the relaxation involves the differential operator - here the divergence one - itself). The result may be obtained using the nonconvex variational approach based on the computation of quasi-convexified function through Young measure (taking advantage of the divergence free form of the equation), see [27]. We refer for instance to [23] for a proof in a similar context. In our simple situation, the result is obtained directly by replacing in the proof of Proposition 3.1, the Haussdorff (compact) convergence for Γ_h^n by the convergence induced by the topology of $L^\infty-\star$ for any minimizing sequence s^n (and using the weak-$\star$ compactness of S_L). □

Theorem 3.1 is very valuable both on theoretical and numerical point of view. First, this result replaces the minimization over domains by a simpler minimization over a set of (density) functions. This in particular avoids the computation of shape derivatives ([6, 16]) and the use of a level set approach (see [2, 20]). Secondly, as we will see in the numerical experiments in Section 5, the property of the optimal density gives valuable information on the nature of the original problem (P_{Γ_h}).

Simpler, the well-posedness of the problem (P_h) is a consequence of the continuity of the solution $\boldsymbol{u}$ with respect to $\boldsymbol{h}$ (see eq. 12) :

PROPOSITION 3.2 *Let $\Gamma_h\neq\emptyset$ be fixed in Γ and $L\in(0,1)$. The problem $(\boldsymbol{P_h})$ admits at least a solution in $(L^2_L(\Gamma_h))^2$.* ■

4 Derivative of $g_{\boldsymbol{\psi}}$ with respect to s and $\boldsymbol{h}$

In order to design a descent algorithm, we derive in this section, for any fixed field $\boldsymbol{\psi} = (\psi_1, 0)$ defined by (10), the explicit expression of the derivatives of $g_{\boldsymbol{\psi}}$ with respect to the variation of $s \in L^\infty(\Gamma, [0,1])$ and $\boldsymbol{h} \in (L^2(\Gamma_h))^2$.

In order to avoid the introduction of a mixed variational formulation and Lagrange multipliers (see for instance [1] in a similar context), we treat the non-interpenetration condition $[\boldsymbol{u} \cdot \boldsymbol{\nu}] \leq 0$ with a penalization technique (see, e.g., [18]). The minimizer of J over $\mathbf{K}$ (solution of (4)–(13)) is approximated by the minimizer (still denoted by $\boldsymbol{u}$) over $(H^1_{\Gamma_0}(\Omega))^2$ of

$$J_\epsilon(\boldsymbol{v}) = J(\boldsymbol{v}) + \epsilon^{-1} \int_\gamma g([\boldsymbol{v}]) d\sigma$$

where g designates a convex function in $C^1(\mathbb{R}^2, \mathbb{R}^+)$ such that $g(\boldsymbol{y}) = 0$ if and only if $\boldsymbol{y} \cdot \boldsymbol{\nu} \leq 0$. A weak solution $\boldsymbol{u} \in (H^1_{\Gamma_0}(\Omega))^2$ is therefore characterized by the following formulation

$$\int_\Omega Tr(\boldsymbol{\sigma}(\boldsymbol{u}) \nabla \boldsymbol{v}) dx + \epsilon^{-1} \int_\gamma \nabla g([\boldsymbol{u}]) \cdot [\boldsymbol{v}] d\sigma = \int_{\Gamma_f} \boldsymbol{f} \cdot \boldsymbol{v} \, d\sigma + \int_{\Gamma_h} \boldsymbol{h} \cdot \boldsymbol{v} \, d\sigma, \quad \forall \boldsymbol{v} \in (H^1_{\Gamma_0}(\Omega))^2.$$

4.1 First variation of $g_{\boldsymbol{\psi}}$ with respect to s and $\boldsymbol{h}$

We introduce a perturbation $s^\eta = s + \eta s_1 \in L^\infty(\Gamma, [0,1])$ of s and we define the first variation of $g_{\boldsymbol{\psi}}$ with respect to s in a standard way:

$$\frac{\partial g_{\boldsymbol{\psi}}(\boldsymbol{u}(s), \boldsymbol{h}, s)}{\partial s} \cdot s_1 = \lim_{\eta \to 0} \frac{g_{\boldsymbol{\psi}}(\boldsymbol{u}(s^\eta), \boldsymbol{h}, s^\eta) - g_{\boldsymbol{\psi}}(\boldsymbol{u}(s), \boldsymbol{h}, s)}{\eta}.$$

The existence of this limit is a consequence of the well-posedness of (RP_{Γ_h}): precisely, we have the following result.

THEOREM 4.1 *The first variation of $g_{\boldsymbol{\psi}}$ with respect to s in the direction $s_1 \in L^\infty(\Gamma, [0,1])$ takes the following expression*

$$\frac{\partial g_{\boldsymbol{\psi}}(\boldsymbol{u}, \boldsymbol{h}, s)}{\partial s} \cdot s_1 = -\int_\Gamma s_1(\boldsymbol{x}) \boldsymbol{h} \cdot \boldsymbol{p} \, d\sigma, \quad \forall s_1 \in L^\infty(\Gamma, [0,1]) \tag{14}$$

where $\boldsymbol{p} \in (H^1_{\Gamma_0}(\Omega))^2$ is solution of the following (weak) adjoint problem:

$$\begin{aligned} \int_\Omega Tr(\boldsymbol{\sigma}(\boldsymbol{p}) \nabla \boldsymbol{\phi}) dx - \int_\Omega Tr(\boldsymbol{\sigma}(\boldsymbol{u}) \nabla \boldsymbol{\phi}) div\, \boldsymbol{\psi} dx + \int_\Omega Tr(\boldsymbol{\sigma}(\boldsymbol{\phi}) \nabla \boldsymbol{u} \nabla \boldsymbol{\psi}) dx \\ + \int_\Omega Tr(\boldsymbol{\sigma}(\boldsymbol{u}) \nabla \boldsymbol{\phi} \nabla \boldsymbol{\psi}) dx + \epsilon^{-1} \int_\gamma \nabla(\nabla g([\boldsymbol{u}]) \cdot [\boldsymbol{\phi}]) \cdot [\boldsymbol{p}] \, d\sigma = 0 \end{aligned} \tag{15}$$

for all $\boldsymbol{\phi} \in (H^1_{\Gamma_0}(\Omega))^2$. ■

Remark 2 *If the crack is oriented along the axis $(O, \boldsymbol{e_1})$, then the radial function ψ_1 defined by (10) verifies the property $\nabla \psi_1 \cdot \boldsymbol{\nu} = 0$ on γ. In this case and assuming the isotropic elasticity (for which $\boldsymbol{\sigma}(\boldsymbol{u}) = \lambda(div \boldsymbol{u}) \mathbf{I} + \mu(\nabla \boldsymbol{u} + \nabla \boldsymbol{u}^T)$, where $\mathbf{I}$ is the identity matrix and (λ, μ) are the Lamé*

coefficients), $\boldsymbol{p} = (p_1, p_2)$ *is formally solution of the following equations:*

$$\begin{cases} -\sigma_{ij,i}(\boldsymbol{p}) + (\sigma_{ij}(\boldsymbol{u})\psi_{1,1})_{,i} - (\sigma_{ij}(\boldsymbol{u})\psi_{1,i})_{,1} \\ \qquad\qquad -\lambda(u_{i,1}\psi_{1,i})_{,j} - \mu((u_{i,1}\psi_{1,j})_{,i} + (u_{j,1}\psi_{1,i})_{,i}) = 0 \quad in \quad \Omega, \\ \boldsymbol{p} = 0 \quad on \quad \Gamma_0, \\ \sigma_{12}(\boldsymbol{p}) = \mu u_{1,2}\psi_{1,1} + \epsilon^{-1}(g_{,11}([\boldsymbol{u}])[p_1] + g_{,12}([\boldsymbol{u}])[p_2]) \quad on \quad \gamma, \\ \sigma_{22}(\boldsymbol{p}) = (\lambda + 2\mu)u_{2,2}\psi_{1,1} + \epsilon^{-1}(g_{,12}([\boldsymbol{u}])[p_1] + g_{,22}([\boldsymbol{u}])[p_2]) \quad on \quad \gamma, \\ \boldsymbol{\sigma}(\boldsymbol{p})\boldsymbol{\nu} = 0 \quad on \quad \partial\Omega\backslash(\Gamma_0 \cup \gamma), \end{cases}$$

and we observe in particular that $\boldsymbol{div}(\boldsymbol{\sigma}(\boldsymbol{p})) = 0$ *on* $\{\boldsymbol{x} \in \Omega, r_1 \leq dist(\boldsymbol{x}, \boldsymbol{F}) \leq r_2\}$. ■

Proof of Theorem 4.1. The expression (14) may be obtained introducing first lagrangian derivatives of $\boldsymbol{u}$ with respect to s and then making integrations by parts (we refer to [16] where the so-called shape derivative of $g_{\boldsymbol{\psi}}$ with respect to Γ_h is computed). For the sake of simplicity, we rather use here the method introduced by J. Cea in [3] which permits to obtain rapidly such derivatives and explain how the formulation (15) of the adjoint solution $\boldsymbol{p}$ is obtained: we introduce the Lagrangian

$$\mathcal{L}(s, \boldsymbol{v}, \boldsymbol{p}) = g_{\boldsymbol{\psi}}(\boldsymbol{v}, \boldsymbol{h}, s) + \int_\Omega Tr(\boldsymbol{\sigma}(\boldsymbol{v})\,\nabla\boldsymbol{p})dx + \epsilon^{-1}\int_\gamma \nabla g([\boldsymbol{v}]) \cdot [\boldsymbol{p}]d\sigma$$
$$- \int_{\Gamma_f} \boldsymbol{f} \cdot \boldsymbol{p}\, d\sigma - \int_\Gamma s(\boldsymbol{x})\boldsymbol{h} \cdot \boldsymbol{p}\, d\sigma,$$

for all $\boldsymbol{v}, \boldsymbol{p} \in (H^1_{\Gamma_0}(\Omega))^2$ and we remark that $\mathcal{L}(\Gamma_h, \boldsymbol{u}, \boldsymbol{p}) = g_{\boldsymbol{\psi}}(\boldsymbol{u}, \boldsymbol{h}, \mathcal{X}_{\Gamma_h})$ for $\boldsymbol{u}$ solution of (4)–(13): formally, we write that

$$\frac{d\mathcal{L}}{ds} \cdot s_1 = \frac{\partial}{\partial s}\mathcal{L}(s, \boldsymbol{v}, \boldsymbol{p}) \cdot s_1 + < \frac{\partial}{\partial \boldsymbol{v}}\mathcal{L}(s, \boldsymbol{v}, \boldsymbol{p}), \frac{\partial \boldsymbol{v}}{\partial s} \cdot s_1 > + < \frac{\partial}{\partial \boldsymbol{p}}\mathcal{L}(s, \boldsymbol{v}, \boldsymbol{p}), \frac{\partial p}{\partial \Gamma_h} \cdot s_1 > .$$

The first term is

$$\frac{\partial}{\partial s}\mathcal{L}(s, \boldsymbol{v}, \boldsymbol{p}) \cdot s_1 = -\int_\Gamma s_1(\boldsymbol{x})\boldsymbol{h} \cdot \boldsymbol{p}\, d\sigma \tag{16}$$

while the third term is equal to zero if $\boldsymbol{v} = \boldsymbol{u}$, due to the linearity of $\mathcal{L}$ with respect to the variable $\boldsymbol{p}$. Introducing to simplify the notation $\frac{\partial \boldsymbol{v}}{\partial s} \cdot s_1 \equiv \boldsymbol{v_1}$ ($\boldsymbol{v_1}$ is the first lagrangian derivative of $\boldsymbol{v}$), we then choose the variable $\boldsymbol{p}$ in order that the second term

$$< \frac{\partial}{\partial v}\mathcal{L}(s, \boldsymbol{v}, \boldsymbol{p}), \boldsymbol{v_1} > = -\frac{1}{2}\int_\Omega Tr(\boldsymbol{\sigma}(\boldsymbol{v})\,\nabla\boldsymbol{v_1})div\boldsymbol{\psi}dx - \frac{1}{2}\int_\Omega Tr(\boldsymbol{\sigma}(\boldsymbol{v_1})\,\nabla\boldsymbol{v})div\boldsymbol{\psi}dx$$
$$+ \int_\Omega Tr(\boldsymbol{\sigma}(\boldsymbol{v})\,\nabla\boldsymbol{v_1}\,\nabla\boldsymbol{\psi})dx + \int_\Omega Tr(\boldsymbol{\sigma}(\boldsymbol{v_1})\,\nabla\boldsymbol{v}\,\nabla\boldsymbol{\psi})dx$$
$$+ \int_\Omega Tr(\boldsymbol{\sigma}(\boldsymbol{v_1})\,\nabla\boldsymbol{p})dx + \epsilon^{-1}\int_\gamma \nabla(\nabla g([\boldsymbol{v}]) \cdot [\boldsymbol{v_1}]) \cdot [\boldsymbol{p}]\, d\sigma$$

is equal to zero for all $\boldsymbol{v_1} \in (H^1_{\Gamma_0}(\Omega))^2$. Using the symmetry of $\boldsymbol{\sigma}$, we write that $Tr(\boldsymbol{\sigma}(\boldsymbol{v})\,\nabla\boldsymbol{v_1}) = Tr(\boldsymbol{\sigma}(\boldsymbol{v_1})\,\nabla\boldsymbol{v})$ and we obtain that $\boldsymbol{p}$ is solution of (15). Then, from (16) with $\boldsymbol{v} = \boldsymbol{u}$ and the relation $\mathcal{L}(\Gamma_h, \boldsymbol{u}, \boldsymbol{p}) = g_{\boldsymbol{\psi}}(\boldsymbol{u}, \boldsymbol{h}, \mathcal{X}_{\Gamma_h})$, we get the relation (14).□

Similarly, assuming Γ_h fixed in Γ, we obtain the first derivative of $g_{\boldsymbol{\psi}}$ with respect to $\boldsymbol{h}$:

THEOREM 4.2 *The first derivative of* $g_{\boldsymbol{\psi}}$ *with respect to* $\boldsymbol{h}$ *in the direction* $\boldsymbol{h_1}$ *is given by*

$$\frac{\partial g_{\boldsymbol{\psi}}(\boldsymbol{u}, \boldsymbol{h}, \mathcal{X}_{\Gamma_h})}{\partial \boldsymbol{h}} \cdot \boldsymbol{h_1} = -\int_{\Gamma_h} \boldsymbol{h_1} \cdot \boldsymbol{p}\, d\sigma, \quad \forall \boldsymbol{h_1} \in (L^2(\Gamma_h))^2 \tag{17}$$

where $\boldsymbol{p}$ *is the solution of (15).* ■

Relations (14) and (17) characterize the minima for the problems (RP_{Γ_h}) and (P_h) respectively. For instance, from (17), the optimal extra load $\boldsymbol{h}$ applied on $\Gamma_h \subset \partial\Omega\backslash(\Gamma_0 \cup \Gamma_f \cup \gamma)$ is such that

$$\boldsymbol{p}(\boldsymbol{u}, \boldsymbol{f}, \Gamma_f, \boldsymbol{h}, \Gamma_h) = 0, \quad \text{on} \quad \Gamma_h,$$

which is a non linear and implicit relation between the optimal extra-load $\boldsymbol{h}$ and the displacement field $\boldsymbol{u}$ on Γ_h, non equal to zero due to the load $\boldsymbol{G}$. These relations also provide descent directions with respect to $\boldsymbol{h}$ and s for $g_{\boldsymbol{\psi}}$ and permit at the numerical level to define gradient algorithms.

4.2 Descent algorithms

4.2.1 Descent algorithm for (RP_{Γ_h})

The relation (14) provides the descent direction $s_1 = \boldsymbol{h} \cdot \boldsymbol{p}$ on Γ and suggests the construction of a sequence of densities $s^{(k)}$ decreasing for $g_{\boldsymbol{\psi}}$. Preliminary, in order to take into account the size restriction on s, i.e., that $\|s\|_{L^1(\Gamma)} = L|\Gamma|$, we introduce a Lagrange multiplier λ and a new cost function:

$$g_{\boldsymbol{\psi},\lambda}(\boldsymbol{u}, \boldsymbol{h}, s) = g_{\boldsymbol{\psi}}(\boldsymbol{u}, \boldsymbol{h}, s) + \lambda(\|s\|_{L^1(\Gamma)} - L|\Gamma|), \quad \forall s \in L^\infty(\Gamma, [0,1])$$

leading to

$$\frac{\partial g_{\boldsymbol{\psi},\lambda}(\boldsymbol{u}, \boldsymbol{h}, s)}{\partial s} \cdot s_1 = -\int_\Gamma s_1(\boldsymbol{x})\boldsymbol{h} \cdot \boldsymbol{p}\, d\sigma + \lambda \int_\Gamma s_1(\boldsymbol{x}) d\sigma$$

and to the descent direction

$$s_1 = \boldsymbol{h} \cdot \boldsymbol{p} - \lambda \quad \text{on} \quad \Gamma. \tag{18}$$

Consequently, for any function $\eta_s \in L^\infty(\Gamma, \mathbb{R}^+)$ with $\|\eta_s\|_{L^1(\Gamma)}$ small enough, we have $g_{\boldsymbol{\psi},\lambda}(\boldsymbol{u}, \boldsymbol{h}, s + \eta_s s_1) \leq g_{\boldsymbol{\psi},\lambda}(\boldsymbol{u}, \boldsymbol{h}, s)$. The multiplier λ is then determined so that, for any function $\eta_s \in L^\infty(\Gamma, \mathbb{R}^+)$, $\|s + \eta_s s_1\|_{L^1(\Gamma)} = L|\Gamma|$, leading to

$$\lambda = \frac{(\int_\Gamma s(\boldsymbol{x}) d\sigma - L|\Gamma|) + \int_\Gamma \eta_s(\boldsymbol{x})\boldsymbol{h} \cdot \boldsymbol{p}\, d\sigma}{\int_\Gamma \eta_s(\boldsymbol{x}) d\sigma}. \tag{19}$$

At last, the function η_s is chosen so that $s + \eta_s s_1 \in [0,1]$, for all $\boldsymbol{x} \in \Gamma$. A simple and efficient choice consists in taking $\eta_s(\boldsymbol{x}) = \varepsilon s(\boldsymbol{x})(1 - s(\boldsymbol{x}))$ for all $\boldsymbol{x} \in \Gamma$ where ε is a small positive parameter.

Consequently, the descent algorithm to solve numerically the relaxed problem (RP_{Γ_h}) may be structured as follows. Let $\Omega \subset \mathbb{R}^2$, Γ_0, Γ_f in $\partial\Omega$, $\boldsymbol{f} \in (L^2(\Gamma_f))^2$, $\boldsymbol{h} \in (L^2(\Gamma_h))^2$, $L \in (0,1)$ and $\varepsilon < 1$, $\varepsilon_1 << 1$ be given ;

- Initialization of the density $s^{(0)} \in L^\infty(\Gamma; (0,1))$;
- For $k \geq 0$, iterate until convergence (i.e. $|g_{\boldsymbol{\psi},\lambda}(\boldsymbol{u}, \boldsymbol{h}, s^{(k+1)}) - g_{\boldsymbol{\psi},\lambda}(\boldsymbol{u}, \boldsymbol{h}, s^{(k)})| \leq \varepsilon_1 |g_{\boldsymbol{\psi},\lambda}(\boldsymbol{u}, \boldsymbol{h}, s^{(0)})|$) as follows:
  - Computation of the solution $\boldsymbol{u}(s^{(k)})$ of (4)–(13) and then the solution $\boldsymbol{p}(s^{(k)})$ of (15), both corresponding to $s = s^{(k)}$.
  - Computation of the descent direction $s_1^{(k)}$ defined by (18) where the multiplier $\lambda^{(k)}$ is defined by (19).
  - Update the density $s^{(k)}$ in Γ:

$$s^{(k+1)} = s^{(k)} + \varepsilon s^{(k)}(1 - s^{(k)}) s_1^{(k)}, \tag{20}$$

  with $\varepsilon \in \mathbb{R}^+$ small enough in order to ensure the decrease of the cost function and $s^{(k+1)} \in L^\infty(\Gamma, [0,1])$.

4.2.2 Descent algorithm for (P_h)

Problem (P_h) is solved in a similar way. In order to ensure $\boldsymbol{h} \in (L^2_L(\Gamma_h))^2$, we introduce the new cost function:

$$g_{\boldsymbol{\psi},\lambda}(\boldsymbol{u},\boldsymbol{h},\mathcal{X}_{\Gamma_h}) = g_{\boldsymbol{\psi}}(\boldsymbol{u},\boldsymbol{h},\mathcal{X}_{\Gamma_h}) + \lambda(\|\boldsymbol{h}\|_{(L^2(\Gamma_h))^2} - L\|\boldsymbol{f}\|_{(L^2(\Gamma_f))^2}).$$

From the relation (17), we deduce that

$$\frac{\partial g_{\boldsymbol{\psi},\lambda}(\boldsymbol{u},\boldsymbol{h},\mathcal{X}_{\Gamma_h})}{\partial \boldsymbol{h}} \cdot \boldsymbol{h_1} = \int_{\Gamma_h} \boldsymbol{h_1} \cdot (-\boldsymbol{p} + 2\lambda \boldsymbol{h})\, d\sigma, \quad \forall \boldsymbol{h_1} \in (L^2(\Gamma_h))^2$$

leading to the descent direction $\boldsymbol{h_1} = (\boldsymbol{p} - 2\lambda\boldsymbol{h})$ so that for any $\varepsilon > 0$ small enough, $g_{\boldsymbol{\psi},\lambda}(\boldsymbol{u},\boldsymbol{h} + \varepsilon(\boldsymbol{p} - 2\lambda\boldsymbol{h}),\Gamma_h) \leq g_{\boldsymbol{\psi},\lambda}(\boldsymbol{u},\boldsymbol{h},\mathcal{X}_{\Gamma_h})$. At last, the multiplier λ is determined so that $\boldsymbol{h} + \varepsilon(\boldsymbol{p} - 2\lambda\boldsymbol{h}) \in (L^2_L(\Gamma_h))^2$; λ is then solution of the polynomial equation of order two:

$$\begin{aligned} 4\varepsilon\|\boldsymbol{h}\|^2_{(L^2(\Gamma_h))^2}\lambda^2 - 4\left(\int_{\Gamma_h} \boldsymbol{p}\cdot\boldsymbol{h} d\sigma + \|\boldsymbol{h}\|^2_{(L^2(\Gamma_h))^2}\right)\lambda \\ - \varepsilon^{-1}(L^2\|\boldsymbol{f}\|^2_{(L^2(\Gamma_f))^2} - \|\boldsymbol{h}\|^2_{(L^2(\Gamma_h))^2}) + 2\int_{\Gamma_h} \boldsymbol{h}\cdot\boldsymbol{p} d\sigma + \varepsilon\|\boldsymbol{p}\|^2_{(L^2(\Gamma_h))^2} = 0. \end{aligned} \tag{21}$$

Observe that the two roots are real if $\varepsilon > 0$ is small enough. The algorithm is then similar to the algorithm of the previous section, (20) being replaced by

$$\boldsymbol{h^{(k+1)}} = \boldsymbol{h^{(k)}} + \varepsilon(\boldsymbol{p}(\boldsymbol{h^{(k)}}) - 2\lambda^{(k)}\boldsymbol{h^{(k)}})$$

where $\lambda^{(k)}$ solves (21).

5 Numerical experiments

We now present some numerical simulations using the algorithm presented above in order to highlight the efficiency of our approach. The systems (3)–(4) and (15) are solved using continuous finite elements of order one approximating the space $H^1_{\Gamma_0}(\Omega)$ by the following finite dimensional space:

$$H^1_{\Gamma_0,h}(\Omega) = \{v_h, v_h \in C^0(\overline{\Omega}), v_h|_Q \in P_1(Q), \forall Q \in Q_h, v_h = 0 \text{ on } \Gamma_0\}, \tag{22}$$

where $P_1(Q)$ denotes the space of polynomial functions of degree ≤ 1 on Q, the notation $(Q_h)_{h>0}$ stands for a regular quasi-uniform family of triangulations (or quadrangulations) (see e.g., [5]) characterized by the space step h such that $\overline{\Omega} = \cup_{Q\in Q_h} Q$. We highlight that the resulted stiffness matrix is identical for the two problems (3)–(4) and (15) and is computed once for all. The lips of the crack γ, assumed rectilinear, are composed of edges of elements in Q_h. Moreover, the non-interpenetration condition on γ: $[\boldsymbol{u}\cdot\boldsymbol{\nu}] \leq 0$ is taken into account using Lagrange multipliers as e.g., in [1, 15, 18], contrary to the section 4 where we used, to simplify the formulae, a penalization term ϵ. This means that in the numerical experiments, the non-interpenetration condition is exactly satisfied. Moreover, we recall that (22) implies the following *a priori* estimation $|G - G_h| = O(h^{1-\eta}), \forall\eta > 0$ if G_h designates the numerical approximation of the rate G provided that the equivalence (8) is used (see [11]).

We consider the structure S occupying the domain $(0,1)^2$ of area 1 square meter, fixed on $\Gamma_0 = \{1\} \times [0,1] = \{\boldsymbol{x} = (x_1,x_2) \in \mathbb{R}^2, x_1 = 1, x_2 \in [0,1]\}$ with a crack $\gamma = [0,0.5] \times \{a\}$, $(a \in (0,1))$, and submitted to the load $\boldsymbol{f} = (f_1,f_2) = (0, 10^6 N/m)$ on $\Gamma_f = [0.3,0.6] \times \{1\}$. We assume that the lower part of S (i.e. $[0,1] \times [0,a]$) is isotropic with a Young modulus E_1 and a

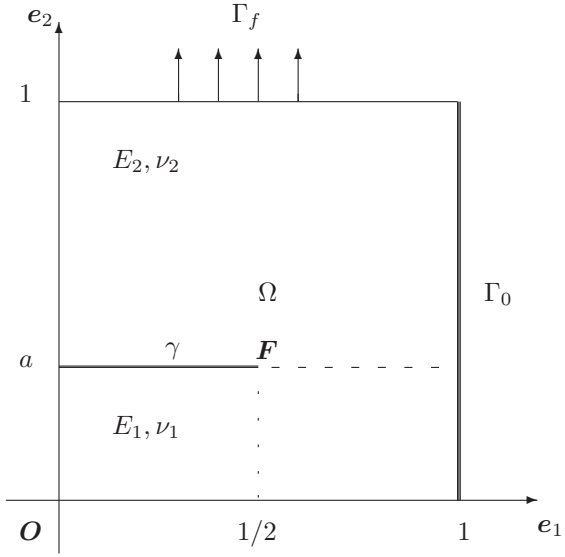

Figure 2: Setting of the problem.

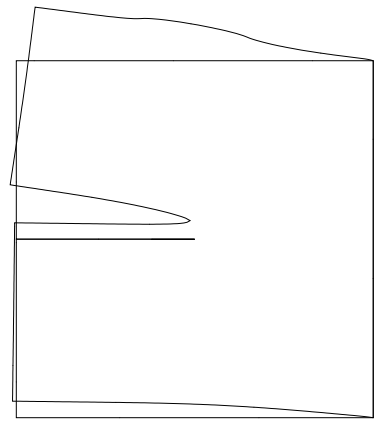

Figure 3: Initial and deformed configurations of S without additional extra force (i.e., $\mathcal{X}_{\Gamma_h} = 0$) and $a = 0.5$: $g_{\boldsymbol{\psi}}(\boldsymbol{u}, \boldsymbol{h}, 0) \approx 1.147 N/m$.

Poisson ratio ν_1 and that the upper part of S (i.e. $[0,1] \times [a,1]$) is isotropic with a Young modulus E_2 and a Poisson ratio ν_2 (see Figure 2).

In all the computations, a quasi uniform mesh of parameter $h = 1/100$ is chosen. In what follows, all the deformed configurations will be depicted with an amplification of 2×10^4.

Consider as an example that the entire body Ω is isotropic with a Young modulus of $2 \times 10^{11} Pa$, a Poisson ratio of 0.3 and a centered crack ($a = 0.5$). The resulted deformation of the structure is shown in Figure 3. As expected, the opening mode (the so-called mode I) is predominant. Moreover, the value of the energy release rate $g_{\boldsymbol{\psi}}$ obtained with ψ_1 defined in (10) (with $r_1 = 0.1$ and $r_2 = 0.4$) is $g_{\boldsymbol{\psi}}(\boldsymbol{u}, \boldsymbol{h}, 0) \approx 1.147 N/m$.

5.1 Problem (RP_{Γ_h})

We now solve problem (RP_{Γ_h}) assuming that $\Gamma = [0,1] \times \{0\}$ (i.e., the lower edge of the structure), $\boldsymbol{h} = (0, h_2)$ with $h_2 = 10^6 N/m$ and $L = 0.3$ so that $\int_\Gamma s(\boldsymbol{x}) h_2 d\sigma = \int_{\Gamma_f} f_2 d\sigma$. The algorithm is initialized with the constant density function $s^{(0)} \equiv L$ in Γ which does not privilege any location for Γ_h, the support of the extra load: therefore, one expects to converge towards a global minimizer of the cost function $g_{\boldsymbol{\psi}}$. Moreover, in what concerns the convergence of the algorithm, we take $\varepsilon_1 = 10^{-4}$ and values of ε varying between 0.05 and 0.3. These values of ε depend on a and on the material characteristics.

5.1.1 $E_1 = E_2 = 2 \times 10^{11} Pa$, $\nu_1 = \nu_2 = 0.3$ and $a = 0.5$.

As mentioned above, the algorithm is initialized with $s^{(0)} = L$ which corresponds to a uniformly distributed normal load $\boldsymbol{h}$ on Γ of intensity $h_2 L$. This particular load reduces the value of the energy rate - we obtain $g_{\boldsymbol{\psi}}(\boldsymbol{u}, \boldsymbol{h}, s^{(0)}) \approx 0.7836 N/m$. However, this load is not optimal: indeed, as we may observe on Figure 6, this load annihilates the mode I (the crack is closed and the contact on the crack lips occurs) but enhances the mode II (the so-called in-plane shear mode). We also

compute that the density $s = \mathcal{X}_{[0.3,0.6]} \in S_L$ corresponding to a symmetric position with respect to Γ_f is not the optimal one: we obtain $g_{\boldsymbol{\psi}}(\boldsymbol{u}, \boldsymbol{h}, s) \approx 0.6203 N/m$. The optimal density s^{opt} for which $g_{\boldsymbol{\psi}}(\boldsymbol{u}, \boldsymbol{h}, s^{opt}) \approx 0.4641 N/m$ obtained at the convergence of the algorithm (after about 150 iterations) is depicted on Figure 4-left. The associated deformation is depicted on Figure 4-right. We observe that this distribution provides a mixed mode I-II situation. Very interestingly on both a mathematical and practical viewpoint, we observe - up to the numerical approximation - that this optimal density s^{opt} is a characteristic function: we get $s^{opt} \approx \mathcal{X}_{[0.42,0.72]}$. This suggests, at least for these data, that the well-posed relaxed problem (RP_{Γ_h}) coincides with the original one (P_{Γ_h}), and therefore, that this latter is well-posed. The evolution of the energy release rate $g_{\boldsymbol{\psi}}$ with respect to the first 100 iterations is shown in Figure 5. A similar satisfactory convergence, which depends actually on ε, is observed in all our computations.

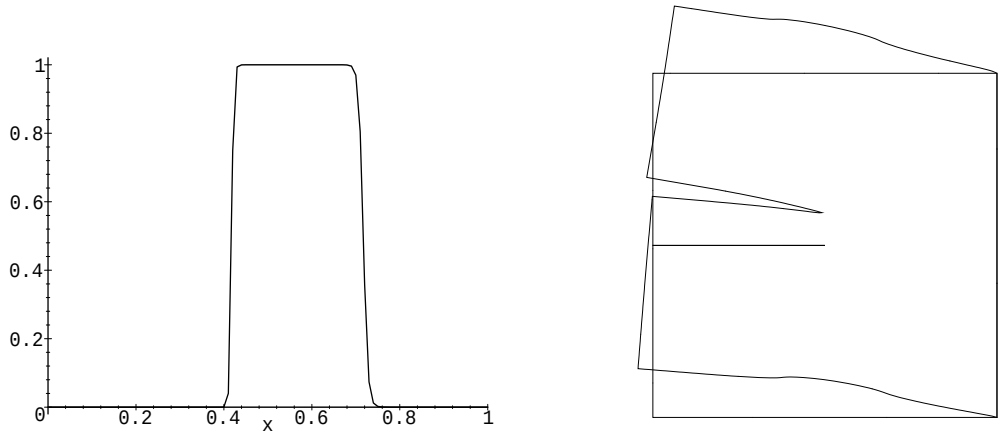

Figure 4: Resolution of (RP_{Γ_h}) - Optimal density s^{opt} (**Left**) and corresponding deformation (**Right**)- $g_{\boldsymbol{\psi}}(\boldsymbol{u}, \boldsymbol{h}, s^{opt}) \approx 0.4641 N/m$.

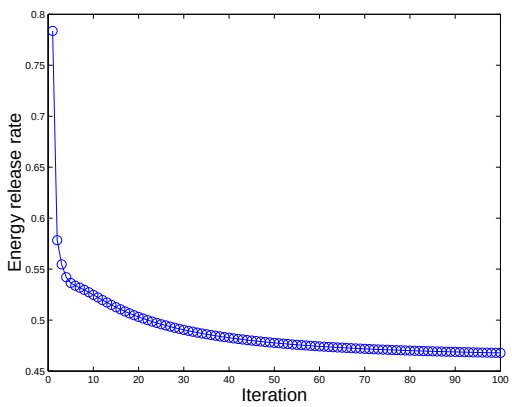

Figure 5: Evolution of $g_{\boldsymbol{\psi}}(\boldsymbol{u}, \boldsymbol{h}, s^{(k)})$ vs. $k \in [1, 100]$ obtained with $\varepsilon = 0.3$.

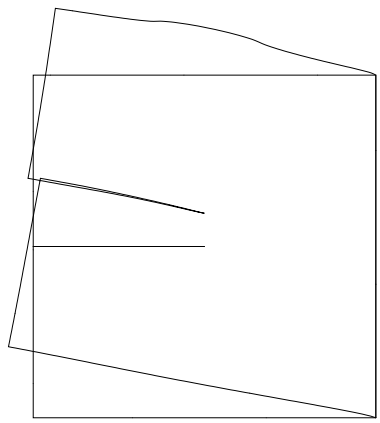

Figure 6: Resolution of (RP_{Γ_h}) - Deformation corresponding to a uniform extra normal load on Γ, i.e. $s^{(0)} = L$ on Γ - $g_{\boldsymbol{\psi}}(\boldsymbol{u}, \boldsymbol{h}, s^{(0)}) \approx 0.7836 N/m$.

5.1.2 $E_1 = E_2 = 2 \times 10^{11} Pa$, $\nu_1 = \nu_2 = 0.3$ and $a = 1/3$.

The same numerical experiment as in 5.1.1 is achieved with a new location of the crack: we take $a = 1/3$ so that $\gamma = [0, 1/2] \times \{1/3\}$. Without additional force, the rate is $g_{\boldsymbol{\psi}}(\boldsymbol{u}, \boldsymbol{h}, 0) \approx 0.3872 N/m$ (obtained with $r_1 = 0.1$ and $r_2 = 0.25$). Choosing a constant $s^{(0)} = L = 0.3$ on Γ as previously, the rate decreases from $0.5876 N/m$ to $0.1050 N/m$ approximatively. Figure 7 shows the optimal distribution of the density and the corresponding deformation of the body. Once again, the limit density is a characteristic function: $s^{opt} \approx \mathcal{X}_{[0.52,0.7] \cup [0.88,1]}$ defined here by two disjoint segments. This last observation highlights the non trivial influence of a on the number of disconnected components of the optimal support Γ_h. We mention that the convergence is particularly slow in this case. More precisely, this result is obtained after 5000 iterations which corresponds in fact to 10000 elasticity problems (5000 nonlinear unilateral contact problems and 5000 linear adjoint problems), each of them having approximately 20000 d.o.f.

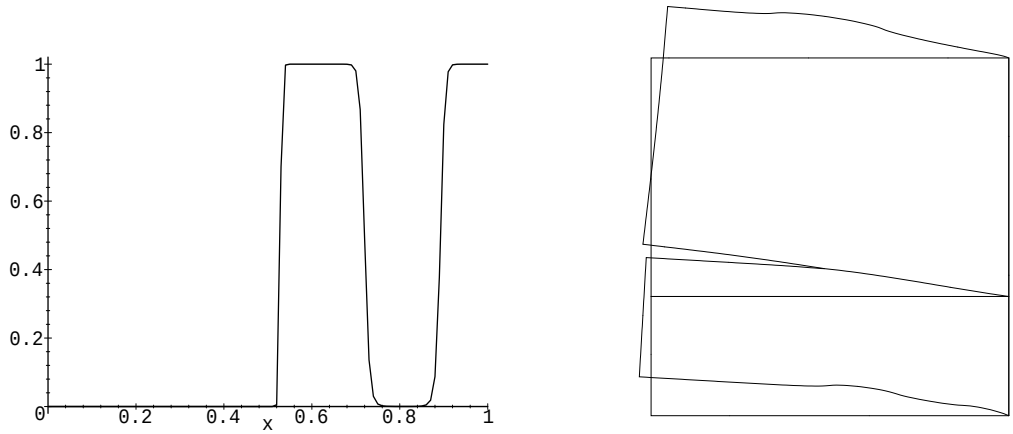

Figure 7: Resolution of (RP_{Γ_h}) - Optimal density s^{opt} (**Left**) and corresponding deformation (**Right**)- $g_{\boldsymbol{\psi}}(\boldsymbol{u}, \boldsymbol{h}, s^{opt}) \approx 0.1050 N/m$.

5.1.3 $E_1 = 2 \times 10^{11} Pa$, $E_2 = 10^{12} Pa$, $\nu_1 = \nu_2 = 0.3$ and $a = 1/2$.

Finally we consider the configuration of 5.1.1 ($a = 1/2$) with a bi-material $E_1 = 2 \times 10^{11} Pa$, $E_2 = 10^{12} Pa$, $\nu_1 = \nu_2 = 0.3$. Without additional force, the rate is equal approximatively to $0.2139 N/m$. Choosing $s^{(0)} = L = 0.3$, the rate decreases from $0.2481 N/m$ to $0.0281 N/m$ approximately. In comparison with the case without additional load, the reduction factor of the rate is about 7.5. Figure 8 shows the optimal distribution of the density and the corresponding deformation of the body: we still get a characteristic function: $s^{opt} \approx \mathcal{X}_{[0.52,0.82]}$.

With $a = 1/2$ and in the isotropic case, we have also considered a non-constant load $\boldsymbol{f}$ in order to see if the resulted optimal density may take value in $(0, 1)$ strictly: precisely, we took $\boldsymbol{f}(x, 1) = (0, (1 - 5x/3) \times 4 \times 10^6 N/m)$ on [0.3,0.6] (note that the L^1-norm of $\boldsymbol{f}$ is unchanged). But here again, the optimal distribution is a characteristic function leading to $\Gamma_h \approx [0.41, 0.71]$.

5.2 Problem (P_h)

We now solve the problem (P_h) with the same data as in Section 5.1 assuming that $\Gamma_h = [0, 1] \times \{0\}$ and that $\boldsymbol{h}$ is normal: $\boldsymbol{h} = (0, h_2)$. We impose that the L^2-norm of the additional load $\boldsymbol{h}$ equals the L^2-norm of $\boldsymbol{f}$: precisely, we require that $\int_{\Gamma_h} (h_2(\boldsymbol{x}))^2 d\sigma = \int_{\Gamma_f} (f_2(\boldsymbol{x}))^2 d\sigma$ which corresponds

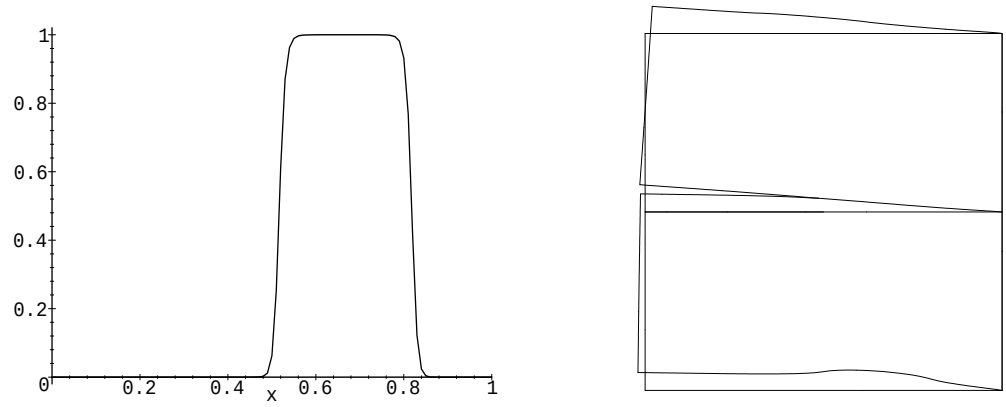

Figure 8: Resolution of (RP_{Γ_h}) - Optimal density s^{opt} (**Left**) and corresponding deformation (**Right**)- $g_{\boldsymbol{\psi}}(\boldsymbol{u}, \boldsymbol{h}, s^{opt}) \approx 0.0281 N/m$.

to $L = 1$ in (6). Note that in the previous section, the L^2-norm was the same for any optimal density (near $\sqrt{0.3}$) because any optimal density was a characteristic function. In other words, in the resolution of both problems (RP_{Γ_h}) and (P_h), the amount of external work applied on the lower part of the structure are equal. Observe however, that in the case of (P_h), no sign or L^∞ bound for h_2 on Γ_h is imposed. Consequently, for a same geometry and elasticity coefficients, the optimal value of the energy release rate, minimized over a larger class of functions, is expected to be lower.

The initial computations are achieved with a constant normal load on Γ_h, i.e. $h_2^{(0)} = |\Gamma_f|^{1/2} f_2 / |\Gamma_h|^{1/2} = \sqrt{0.3} f_2$ for which $\boldsymbol{h^{(0)}} = (0, h_2^{(0)}) \in (L^2_{L=1}(\Gamma_h))^2$. We next consider the configurations of Section 5.1.1, 5.1.2 and 5.1.3.

5.2.1 $E_1 = E_2 = 2 \times 10^{11} Pa$, $\nu_1 = \nu_2 = 0.3$ and $a = 1/2$.

The initial computation leads to the value $g_{\boldsymbol{\psi}}(\boldsymbol{u}, \boldsymbol{h^{(0)}}, \mathcal{X}_{\Gamma_h}) \approx 1.5927 N/m$. Figure 9-left gives the

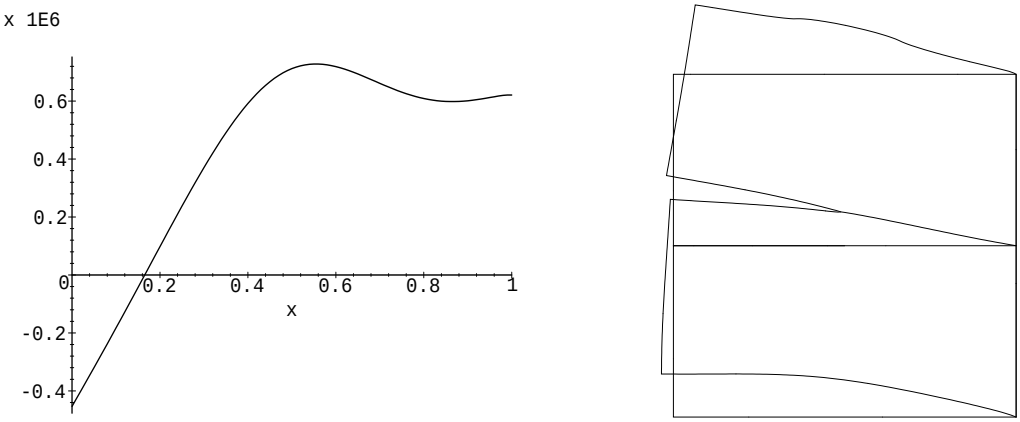

Figure 9: Resolution of (P_h) - Optimal density h_2^{opt} (**Left**) and corresponding deformation (**Right**)- $g_{\boldsymbol{\psi}}(\boldsymbol{u}, \boldsymbol{h}^{opt}, \mathcal{X}_{\Gamma_h}) \approx 0.4328 N/m$.

optimal distribution of h_2^{opt} which provides a value of the energy release rate of $g_{\boldsymbol{\psi}}(\boldsymbol{u}, (0, h_2^{opt}), \mathcal{X}_{\Gamma_h}) \approx$

$0.4328N/m$. The corresponding deformation is depicted in Figure 9-right. As expected the optimal rate is lower than the one in section 5.1.1 (i.e., $0.4641N/m$) where the L^2 norm of $\boldsymbol{h}$ was the same. The optimal load illustrates clearly the balance between the mode I and the mode II. On a large right part of Γ_h, the load is positive, which has the effect to close the crack and therefore to reduce the contribution of the mode I on the value of the rate. On the left extremity of Γ_h, the load is negative; this gives the effect to reduce the in-plane shear of the crack lips and therefore the contribution of the mode II (see Figure 6 for the effect of a strictly positive load).

5.2.2 $E_1 = E_2 = 2 \times 10^{11} Pa$, $\nu_1 = \nu_2 = 0.3$ and $a = 1/3$.

Now we consider problem (P_h) with the configuration of 5.1.2. In this case the rate decreases from $1.1948N/m$ to $0.0353N/m$. Recalling that the rate without additional force was $0.3872N/m$ we observe a reduction of order 10. Figure 10 shows the optimal distribution of the density and the corresponding deformation of the body. Contrary to the problem (RP_{Γ_h}), the optimal load is less sensitive here to the position of the crack.

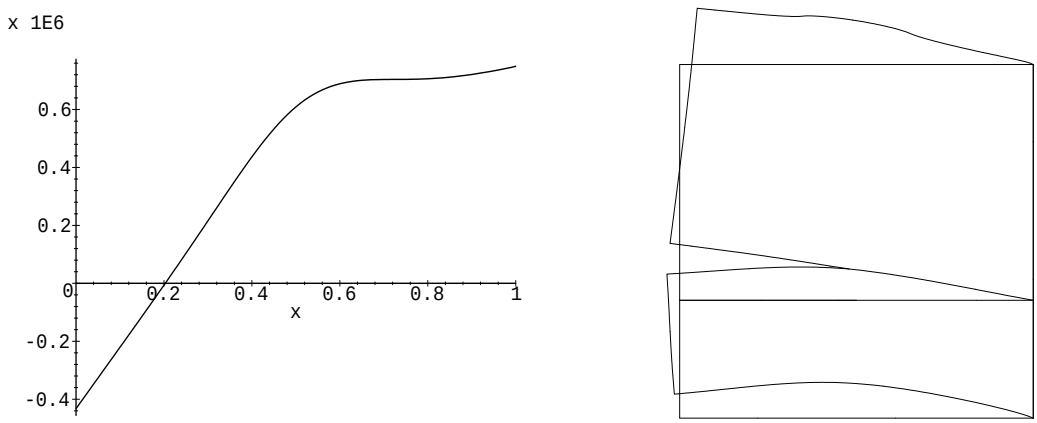

Figure 10: Resolution of (P_h) - Optimal density h_2^{opt} (**Left**) and corresponding deformation (**Right**)- $g_{\boldsymbol{\psi}}(\boldsymbol{u}, \boldsymbol{h}^{opt}, \mathcal{X}_{\Gamma_h}) \approx 0.0353N/m$.

5.2.3 $E_1 = 2 \times 10^{11} Pa$, $E_2 = 10^{12} Pa$, $\nu_1 = \nu_2 = 0.3$ and $a = 1/2$.

Finally we consider problem (P_h) for the configuration in 5.1.3: the rate decreases from $0.4799N/m$ to $0.00679N/m$. We observe a reduction of order 30 in comparison with the initial problem for which the rate is $0.2139N/m$. Figure 11 shows the optimal distribution of the density and the corresponding deformation of S.

5.2.4 $E_1 = E_2 = 2 \times 10^{11} Pa$, $\nu_1 = \nu_2 = 0.3$ and $a = 1/2$, without constraint on $\boldsymbol{h}$.

We finally examine if a load in $(L^2(\Gamma_h))^2$ without any additional constraint may annihilate the energy release rate and therefore the singularities around the crack extremities $\boldsymbol{F} = (1/2, 1/2)$. We consider the isotropic situation with a centered crack. Results obtained after 1500 iterations (with $\varepsilon = 0.3$) are reported on Figure 12. We obtain the value $g_{\boldsymbol{\psi}}(\boldsymbol{u}, \boldsymbol{h}^{opt}, \mathcal{X}_{\Gamma_h}) \approx 0.0383N/m$ (corresponding to a reduction of order 30). Obviously this value is obtained with a larger L^∞ norm of the load (in a ratio 10) than in the previous cases. Around the crack point $\boldsymbol{F}$, the crack lips are closed without in plane shear. However, the evolution of the algorithm seems to indicate

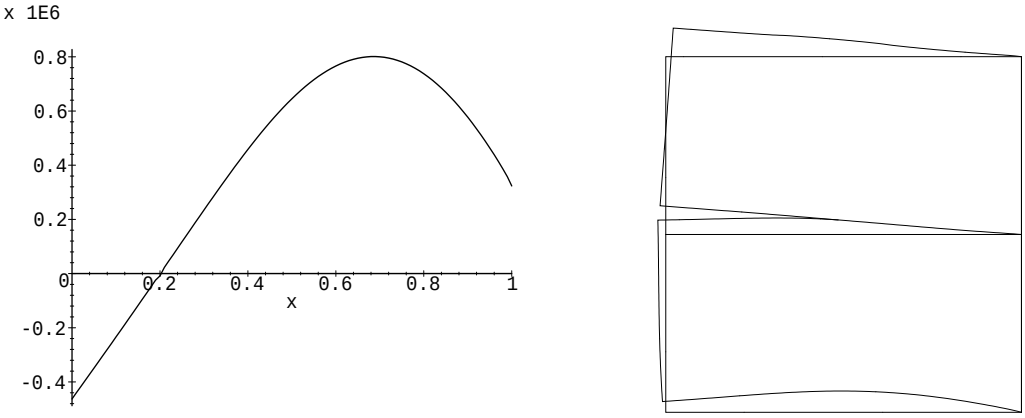

Figure 11: Resolution of (P_h) - Optimal density h_2^{opt} (**Left**) and corresponding deformation (**Right**) - $g_{\boldsymbol{\psi}}(\boldsymbol{u}, \boldsymbol{h}^{opt}, \mathcal{X}_{\Gamma_h}) \approx 0.00679 N/m$.

that an arbitrarily small value of the rate (ideally $g_{\boldsymbol{\psi}} = 0$) may be difficult to obtain: we suspect that a small tangential component of the force is necessary to near $g_{\boldsymbol{\psi}} = 0$ and therefore to almost cancel the singularity at the point $\boldsymbol{F}$.

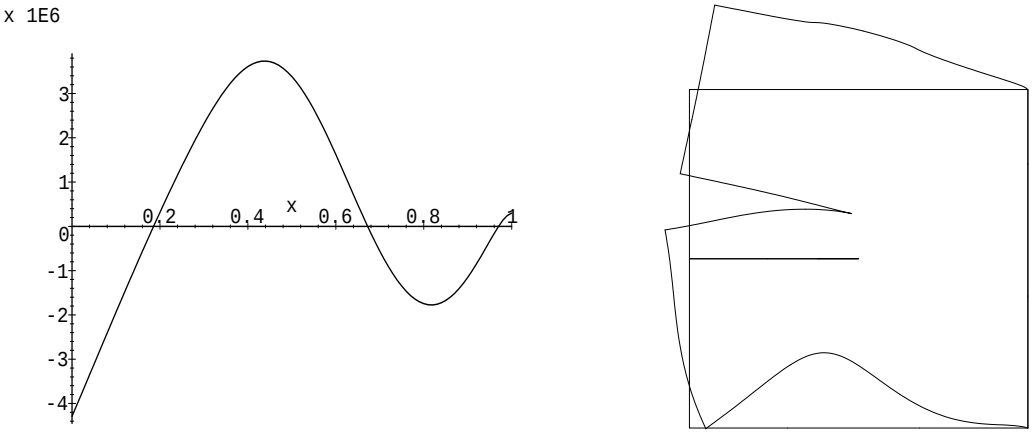

Figure 12: Resolution of (P_h) without constraint on $\boldsymbol{h}$- Optimal density h_2^{opt} (**Left**) and corresponding deformation (**Right**) - $g_{\boldsymbol{\psi}}(\boldsymbol{u}, \boldsymbol{h}^{opt}, \mathcal{X}_{\Gamma_h}) \approx 0.0383 N/m$.

5.3 The case of two cracks

We consider in this section the problem (P_{Γ_h}) for the unit square with two cracks $\gamma_1 = [0, a_1] \times \{1/4\}$ and $\gamma_2 = [0, a_2] \times \{1/2\}$ of extremities $\boldsymbol{F_1} = (a_1, 1/4)$ and $\boldsymbol{F_2} = (a_2, 1/2)$ respectively. The energy release $g_{\boldsymbol{\psi}}$ is then the sum of the energy release rate $g_{\boldsymbol{\psi}^{(i)}}$ associated with each crack point $\boldsymbol{F_i}$, $i = 1, 2$: the first component of the function $\boldsymbol{\psi} = (\psi_1^{(1)} + \psi_1^{(2)}, 0)$ is the sum of two functions of the form (10) with disjoint supports in the neighborhoods of $\boldsymbol{F_1}$ and $\boldsymbol{F_2}$ respectively. We take $E_1 = E_2 = 2 \times 10^{11}$, $\nu_1 = \nu_2 = 0.3$, $\boldsymbol{h} = (0, h_2)$, $h_2 = 10^6 N/m$ and $L = 0.3$. We consider three configurations corresponding to $(a_1, a_2) = (1/4, 1/2)$, $(a_1, a_2) = (1/2, 1/2)$ and $(a_1, a_2) =$

$(1/2, 1/4)$. The densities obtained at the convergence of the gradient algorithm (initialized with $s^{(0)} \equiv L = 0.3$) are depicted on Figure 13 as well as the corresponding deformations of the structure. Some numerical values are collected in Table 1 which illustrate the reduction of the energy release rate as well as the Von Mises stress around the crack tips (we recall that the energy release rate is a measure of the displacement's singularity around the crack tip, here $\boldsymbol{F_1}$ and $\boldsymbol{F_2}$ (see Remark 1)). Figure 13 highlights the respective influence of the two cracks. When $a_1 \leq a_2$, the lower crack γ_1 is hidden from the load $\boldsymbol{f}$ by the second crack γ_2, which is the main contribution to the energy release rate (the Von Mises stress associated to $\boldsymbol{F_1}$ is significantly lower in this case, see Table 1). The situation is opposite is the third case $(a_1, a_2) = (1/2, 1/4)$ so that the crack γ_1 is not closed: due to the balance between mode I and mode II observed in the previous section, we remark that the corresponding optimal density is mainly concentrated on the right part of the side $[0, 1] \times \{0\}$, support of the extra-load $\boldsymbol{h}$. In the case $(a_1, a_2) = (1/2, 1/4)$, Figure 15 depicts the iso-values of the Von Mises stresses and permits to appreciate the reduction of the stresses near the crack tips $\boldsymbol{F_1}$ and $\boldsymbol{F_2}$. Remark that the singularities of the stresses at the corners $(1, 0)$ and $(1, 1)$ are due to the Dirichlet-Neumann transition. The regularity for $\boldsymbol{u}$ at the corners (in the homogeneous case which corresponds to point $(1, 1)$ or to both corners in the case without extra force) is of order $H^{3/2+\epsilon}$ (see [26, 28]) which is close to the regularity near the crack tip which is $H^{3/2-\epsilon}$ for any $\epsilon > 0$.

The main difference with respect to the single crack situation is that the densities are no more characteristic functions. This illustrates either that these densities in Figure 13 correspond to local minima, or that problem (P_{Γ_h}) is not well-posed (for this geometric configuration). In this last case, from a practical point of view, it is then necessary to associate with each density, a minimizing sequence of characteristic functions for (P_{Γ_h}) (as described in Theorem 3.1). Using [23], the procedure is as follows : the interval $[0, 1]$ is decomposed into $k > 0$ sub-intervals $[0, 1] = \cup_{j=1}^{k}[x_j, x_{j+1}]$ such that $x_1 = 0$ and $x_{k+1} = 1$. Then, we define a mean value $m_j \in [0, 1]$ by $m_j = \int_{x_j}^{x_{j+1}} s^{lim}(x)dx/(x_{j+1} - x_j)$. The sequence of characteristic functions $(\mathcal{X}_{\Gamma_h^{(k)}})_{k>0}$ is then defined by

$$\mathcal{X}_{\Gamma_h^{(k)}}(x) = \sum_{j=1}^{k} \mathcal{X}_{[x_j,(1-m_j)x_j+m_jx_{j+1}]}(x), \quad x \in \Gamma = [0, 1] \times \{0\}. \tag{23}$$

We easily check that $\mathcal{X}_{\Gamma_h}^{(k)}$ belongs to $\mathcal{X}_L$ for all k. The support of the extra load $\boldsymbol{h}$ is then $\cup_{i=1}^{k}[x_j, (1-m_j)x_j + m_jx_{j+1}]$. At the limit, the force is distributed on an arbitrarily large number of disjoint intervals. Figure 14 displays the case $k = 10$ associated to the limit density s^{lim} for $(a_1, a_2) = (1/2, 1/2)$: we compute that $g_{\boldsymbol{\psi}}(\boldsymbol{u}, \boldsymbol{h}, \mathcal{X}_{\Gamma_h}^{(10)}) \approx 0.669N/m$, which is almost the value of the rate associated with the limit density: this suggests the existence of several global/local minima and that the optimal support of the extra force may be recovered by a characteristic function (in other words, this suggests that (P_{Γ_h}) is also well-posed in that case).

We finally consider the problem (P_h) for the case $(a_1, a_2) = (1/2, 1/4)$. The normal component h_2^{opt} of the optimal load and the corresponding deformation are given on Figure 16. This load permits a significant reduction of the rate : we get $g_{\boldsymbol{\psi}}(\boldsymbol{u}, h^{opt}, \mathcal{X}_{\Gamma_h}) \approx 0.0556N/m$. We also observe a significant reduction of the Von Mises stress at the crack tip $\boldsymbol{F_1}$: $\sigma_{VM}(\boldsymbol{F_1}, h_2^{opt}, \mathcal{X}_{\Gamma_h}) \approx 7.6\times10^5 Pa$ (to be compared with the case without extra load for which $\sigma_{VM}(\boldsymbol{F_1}, \boldsymbol{0}, \mathcal{X}_{\Gamma_h}) \approx 2.1\times10^6 Pa$ - see also Figure 15- Bottom) while the second tip $\boldsymbol{F_2}$ is less perturbed ($\sigma_{VM}(\boldsymbol{F_2}, h_2^{opt}, \mathcal{X}_{\Gamma_h}) \approx 9.1 \times 10^5 Pa$).

6 Concluding remarks

In this work we have considered two optimal control problems whose aim is to prevent the crack growth by searching "optimal" boundary loads. As far as we know these problems have not

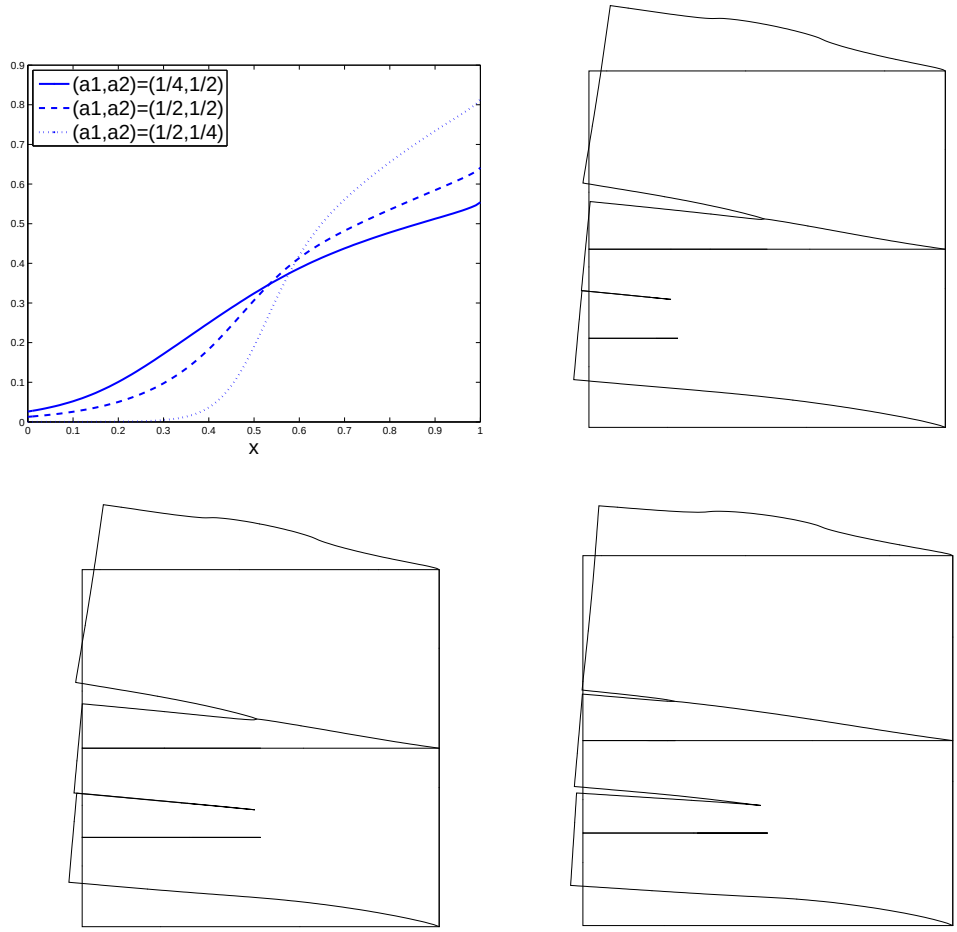

Figure 13: Resolution of (RP_{Γ_h}) - Limit densities (**top left**) and corresponding deformation for $(a_1, a_2) = (1/4, 1/2)$ (**top right**), $(a_1, a_2) = (1/2, 1/2)$ (**bottom left**) and $(a_1, a_2) = (1/2, 1/4)$ (**bottom right**).

	$(a_1, a_2) = (1/4, 1/2)$	$(a_1, a_2) = (1/2, 1/2)$	$(a_1, a_2) = (1/2, 1/4)$
$g_{\boldsymbol{\psi}}(\boldsymbol{u}, \boldsymbol{h}, 0)$	1.151	1.152	0.232
$g_{\boldsymbol{\psi}}(\boldsymbol{u}, \boldsymbol{h}, s^{(0)})$	0.861	1.49	0.461
$g_{\boldsymbol{\psi}}(\boldsymbol{u}, \boldsymbol{h}, s^{lim})$	0.582	0.668	0.102
$\sigma_{VM}(\boldsymbol{F_1}, \boldsymbol{h}, 0)$	4.7×10^4	5.2×10^5	2.1×10^6
$\sigma_{VM}(\boldsymbol{F_1}, \boldsymbol{h}, s^{(0)})$	7.6×10^5	4.2×10^6	3.8×10^6
$\sigma_{VM}(\boldsymbol{F_1}, \boldsymbol{h}, s^{lim})$	2.1×10^5	1.2×10^6	1.4×10^6
$\sigma_{VM}(\boldsymbol{F_2}, \boldsymbol{h}, 0)$	4.5×10^6	4.4×10^6	8.4×10^5
$\sigma_{VM}(\boldsymbol{F_2}, \boldsymbol{h}, s^{(0)})$	$5. \times 10^6$	5.7×10^6	1.5×10^6
$\sigma_{VM}(\boldsymbol{F_2}, \boldsymbol{h}, s^{lim})$	4.2×10^6	4.2×10^6	9.1×10^5

Table 1: Numerical values of the energy release rate (in N/m) and of the Von Mises stresses (in Pa) around the crack tips $\boldsymbol{F_1}$ and $\boldsymbol{F_2}$ (see Figure 13).

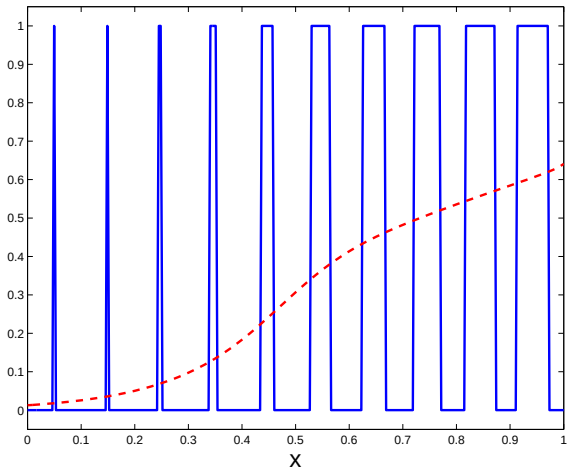

Figure 14: Penalization of the limit density s^{lim} in the case $(a_1, a_2) = (1/2, 1/2)$ by a characteristic function $\mathcal{X}^{(10)}_{\Gamma_h}$.

been investigated previously. Although this study of *active crack control* should be considered as preliminary in many respects, the results obtained have some valuable implications and lead to interesting observations, both from a mathematical and a mechanical viewpoint. The numerical method we have proposed, based on first gradient and descent direction, appears robust and provides after the iterative process a minimum of the energy release rate. The main difficulty - but nowadays well addressed in the literature - is the unilateral contact condition on the crack lips. From a mechanical viewpoint, the numerical simulations exhibit the interplay between the opening mode (mode I) and the in-plane shear mode (mode II), interplay which produces in some situations non trivial optimal positions or amplitudes for the extra force. In three dimensional cases, the situation is expected to be more complex and interesting with the apparition of the mode III (out-of-plane shear mode). We also observe that the extra force - restricted to upper bound on the L^2-norm - permits to reduce significantly the rate and therefore prevents or at least reduces the possible crack growth. When no condition is imposed on the amplitude of the additional force, we check that the rate may be driven to a very small value. Moreover, from the numerical experiments, we may conjecture that the design problem (P_{Γ_h}) is always well-posed, i.e. that the optimal support Γ_h is composed of a finite number of disjoint components, and therefore easily designed in practice.

Furthermore, we point out that the method and arguments used here extend directly to more general cases, including tangential additional load, internal crack on complex geometries and also curved cracks or curved boundaries (see [21, 22]). The case of the contact with Coulomb friction, more challenging, is also worth to be investigated. Finally, we plan to address the similar problem which consists in optimizing the distribution of two isotropic materials on the structure Ω in order to reduce the corresponding energy release rate (we refer to [24] for the scalar case).

Acknowledgments - The authors thank Philippe Destuynder (CNAM, Paris) for interesting discussions related to this work.

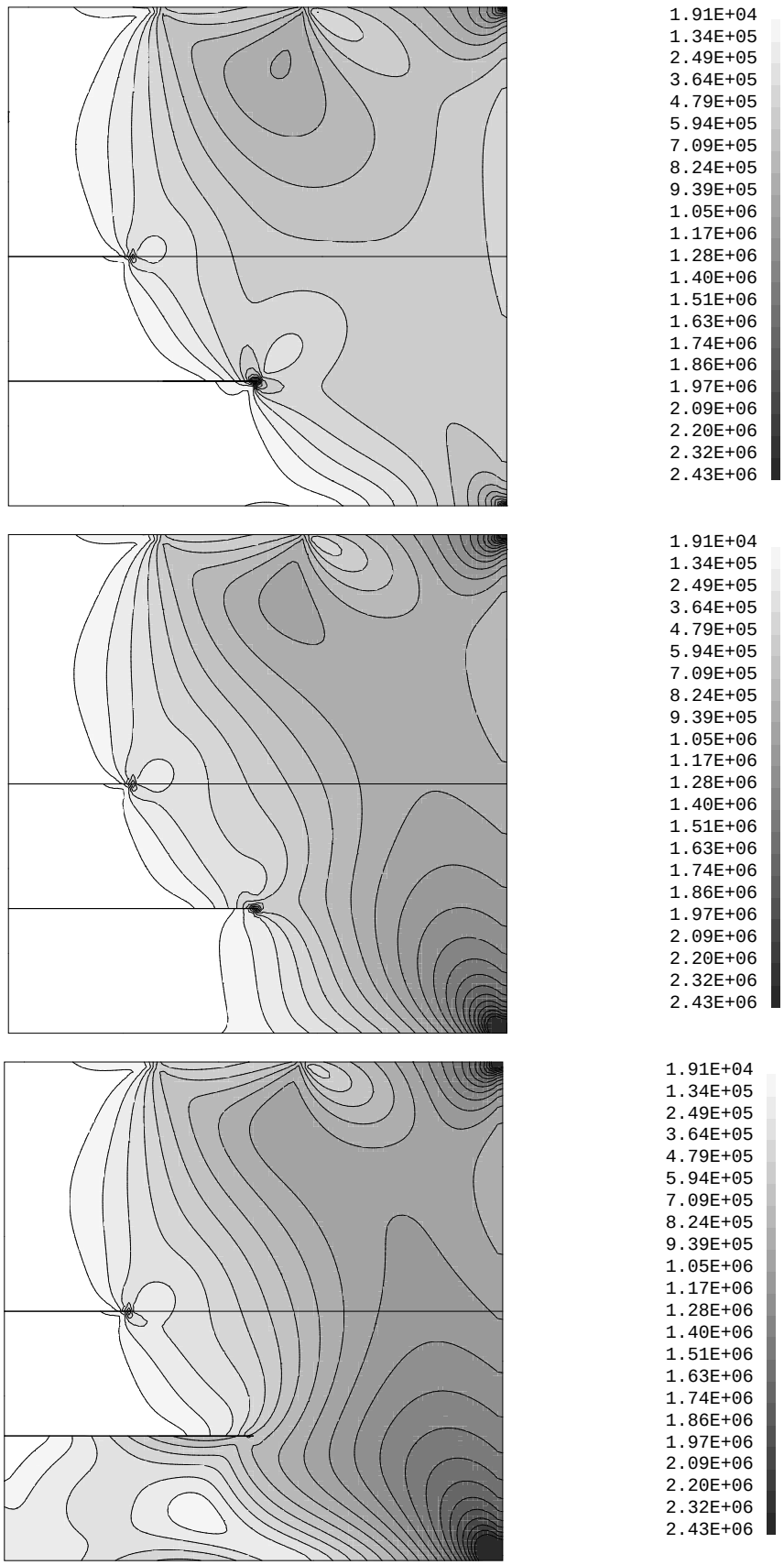

Figure 15: Iso-values of the Von Mises Stresses on Ω - **a)** without extra-force $g_{\boldsymbol{\psi}}(\boldsymbol{u}, \boldsymbol{h}, 0) \approx 0.232N/m$ (**Top**) - **b)** from (RP_{Γ_h}) $g_{\boldsymbol{\psi}}(\boldsymbol{u}, \boldsymbol{h}, s^{opt}) \approx 0.102N/m$ (**Mid**) and **c)** from (P_h) $g_{\boldsymbol{\psi}}(\boldsymbol{u}, \boldsymbol{h}^{opt}, \mathcal{X}_{\Gamma_h}) \approx 0.0556N/m$ (**Bottom**).

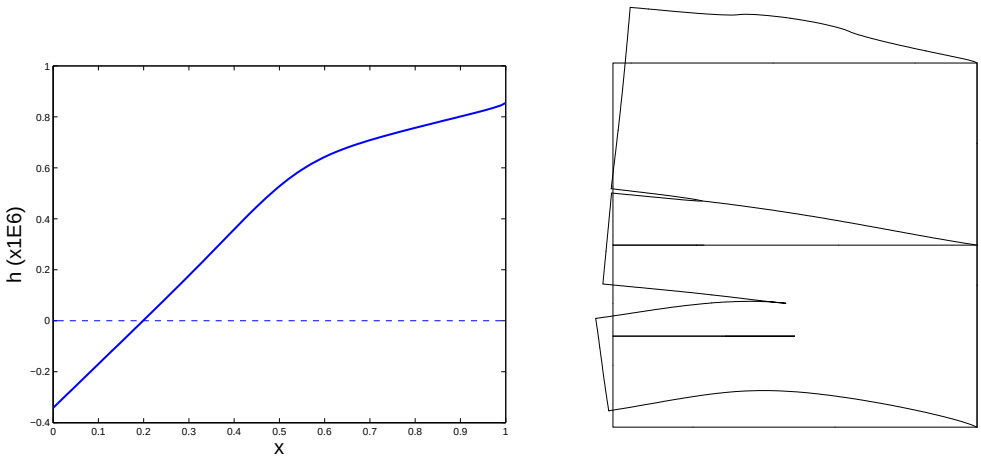

Figure 16: Resolution of (P_h) - Optimal density h_2^{opt} (**Left**) and corresponding deformation (**Right**) - $g_\psi(\boldsymbol{u}, \boldsymbol{h}^{opt}, \mathcal{X}_{\Gamma_h}) \approx 0.0556 N/m$.

References

[1] Z. Belhachmi, J.M. Sac-Epée, J. Sokolowski, *Mixed finite element methods for smooth domain formulation of crack problems*, SIAM J. Numer. Anal. **43** (2005) 1295–1320.

[2] M. Burger, S. Osher, *A survey on levet set methods for inverse problems and optimal design*, European J. Appl. Math., **16** (2005) 263–301.

[3] J. Cea, *Conception optimale ou identification de formes, calcul rapide de la dérivée directionnelle de la fonction coût*, Math. Model. Numer. Anal., **20** (1986) 371–402.

[4] J.L. Chaboche, J. Lemaitre, *Mécanique des matériaux solides*, Dunod, Paris, 1985.

[5] P.G. Ciarlet, *The finite element method for elliptic problems*, in Handbook of Numerical Analysis, Volume II, Part 1, eds. P.G. Ciarlet and J.L. Lions, North Holland, pp. 17–352, 1991.

[6] M.C. Delfour, J.-P. Zolesio, *Shapes and Geometries - Analysis, Differential Calculus and Optimization*, Advances in Design and Control, SIAM, 2001.

[7] P. Destuynder, *Calculation of forward thrust of a crack, taking into account the unilateral contact between the lips of the crack*, C. R. Acad. Sci. Paris, Série II, **296** (1983) 745–748.

[8] P. Destuynder, *An approach to crack propagation control in structural dynamics*, C. R. Acad. Sci. Paris, Série II, **306** (1988) 953–956.

[9] P. Destuynder, *Remarks on a crack propagation control for stationary loaded structures*, C. R. Acad. Sci. Paris, Série IIb, **308** (1989) 697–701.

[10] P. Destuynder, *Computation of an active control in fracture mechanics using finite elements*, Eur. J. Mech., A/Solids, **9** (1990) 133–141.

[11] P. Destuynder, M. Djaoua, S. Lescure, *Quelques remarques sur la mécanique de la rupture élastique* , J. Méca. Théor. Appli, **2** (1983) 113–135.

[12] G.A. Francfort, J.J. Marigo, *Revisiting brittle fracture as an energy minimisation problem*, J. Mech. Phys. Solids, **46** (1998) 1319–1342.

[13] A.A. Griffith, *The phenomena of rupture and flow in Solids*, Phil. Trans. Roy. Soc. London, **46** (1920) 163–198.

[14] A. Henrot, M. Pierre, *Variation et optimisation de formes*, Mathématiques et Applications **48**, Springer (2005) pp 1-334.

[15] P. Hild, *Numerical implementation of two nonconforming finite element methods for unilateral contact*, Comput. Methods Appl. Mech. Engrg., **184** (2000) 99–123.

[16] P. Hild, A. Münch, Y.Ousset, *On the control of crack growth in elastic media*, C. R. Acad. Sci. Paris, Série IIb, **36(5)**, (2008) 22-27.

[17] A.M. Khludnev, J. Sokolowski, *Modelling and control in solid mechanics*. International Series of Numerical Mathematics, **122**, Birkhäuser Verlag, Basel, 1997.

[18] N. Kikuchi, J.T. Oden, *Contact problems in elasticity*, SIAM, Philadelphia, 1988.

[19] J-B. Leblond, *Mécanique de la rupture fragile et ductile*, Hermes, Paris, 2003.

[20] A. Münch, *Optimal design of the support of the control for the 2-D wave equation: numerical investigations*, Int. J. Numerical Analysis and Modeling, **5** (2008) 331–351.

[21] A. Münch, Y. Ousset, *Energy release rate for a curvilinear beam*, C. R. Acad. Sci. Paris, Série IIb, **328** (2000) 471–476.

[22] A. Münch, Y. Ousset, *Numerical simulation of delamination growth in curved interfaces*, Comput. Methods Appl. Mech. Engrg, **191** (2002) 2045–2067.

[23] A. Münch, P. Pedregal, F. Periago, *Optimal design of the damping set for the stabilization of the wave equation*, J. Diff. Eq., **231** (2006) 331–358.

[24] A. Münch, P. Pedregal, *Relaxation of an optimal design problem in fracture mechanic*, Preprint Université Franche-Comté 03-08, January 08.

[25] M.T. Niane, G. Bayili, A. Sène, M. Sy, *Is it possible to cancel singularities in a domain with corners and cracks ?* C. R. Acad. Sci. Paris, Série I, **343** (2006) 115–118.

[26] S. Nicaise, *About the Lamé system in a polygonal or a polyhedral domain and a coupled problem between the Lamé system and the plate equation. I: Regularity of the solutions,* Ann. Scuola Norm. Sup. Pisa Cl. Sci., **19** (1992) 327–361.

[27] P. Pedregal, *Vector variational problems and applications to optimal design*, Esaim: Cocv, **11** (2005) 357–381.

[28] A. Rössle, *Corner singularities and regularity of weak solutions for the two-dimensional Lamé equations on domains with angular corners*, Journal of Elasticity, **60** (2000) 57–75.